

Gel-Dispersed Nanostructured Lipid Carriers Loading Thymol Designed for Dermal Pathologies

Camila Folle¹, Ana M Marqués², Natalia Díaz-Garrido³⁻⁵, Paulina Carvajal-Vidal¹, Elena Sánchez López^{1,6}, Joaquim Suñer-Carbó^{1,6}, Lyda Halbaut^{1,6}, Mireia Mallandrich^{1,6}, Marta Espina^{1,6}, Josefa Badia³⁻⁵, Laura Baldoma³⁻⁵, Maria Luisa García^{1,6}, Ana Cristina Calpena^{1,6}

¹Department of Pharmacy and Pharmaceutical Technology and Physical Chemistry, Faculty of Pharmacy and Food Sciences, University of Barcelona, Barcelona, Spain; ²Department of Biology, Healthcare and Environment, Faculty of Pharmacy and Food Sciences, University of Barcelona, Barcelona, Spain; ³Department of Biochemistry and Physiology, Faculty of Pharmacy and Food Sciences, University of Barcelona, Barcelona, Spain; ⁴Institute of Biomedicine of the University of Barcelona (IBUB), Barcelona, Spain; ⁵Research Institute Sant Joan De Déu (IR-SJD), Barcelona, Spain; ⁶Institute of Nanoscience and Nanotechnology (IN2UB), University of Barcelona, Barcelona, Spain

Correspondence: Camila Folle; Elena Sánchez López, Department of Pharmacy and Pharmaceutical Technology and Physical Chemistry, Faculty of Pharmacy and Food Sciences, University of Barcelona, Barcelona, 08028, Spain, Email camilafolle@ub.edu; esanchezlopez@ub.edu

Purpose: *Acne vulgaris* is one of the most prevalent dermal disorders affecting skin health and appearance. To date, there is no effective cure for this pathology, and the majority of marketed formulations eliminate both healthy and pathological microbiota. Therefore, hereby we propose the encapsulation of an antimicrobial natural compound (thymol) loaded into lipid nanostructured systems to be topically used against acne.

Methods: To address this issue, nanostructured lipid carriers (NLC) capable of encapsulating thymol, a natural compound used for the treatment of acne vulgaris, were developed either using ultrasonication probe or high-pressure homogenization and optimized using 2²-star factorial design by analyzing the effect of NLC composition on their physicochemical parameters. These NLC were optimized using a design of experiments approach and were characterized using different physicochemical techniques. Moreover, short-term stability and cell viability using HaCat cells were assessed. Antimicrobial efficacy of the developed NLC was assessed in vitro and ex vivo.

Results: NLC encapsulating thymol were developed and optimized and demonstrated a prolonged thymol release. The formulation was dispersed in gels and a screening of several gels was carried out by studying their rheological properties and their skin retention abilities. From them, carbomer demonstrated the capacity to be highly retained in skin tissues, specifically in the epidermis and dermis layers. Moreover, antimicrobial assays against healthy and pathological skin pathogens demonstrated the therapeutic efficacy of thymol-loaded NLC gelling systems since NLC are more efficient in slowly reducing *C. acnes* viability, but they possess lower antimicrobial activity against *S. epidermidis*, compared to free thymol.

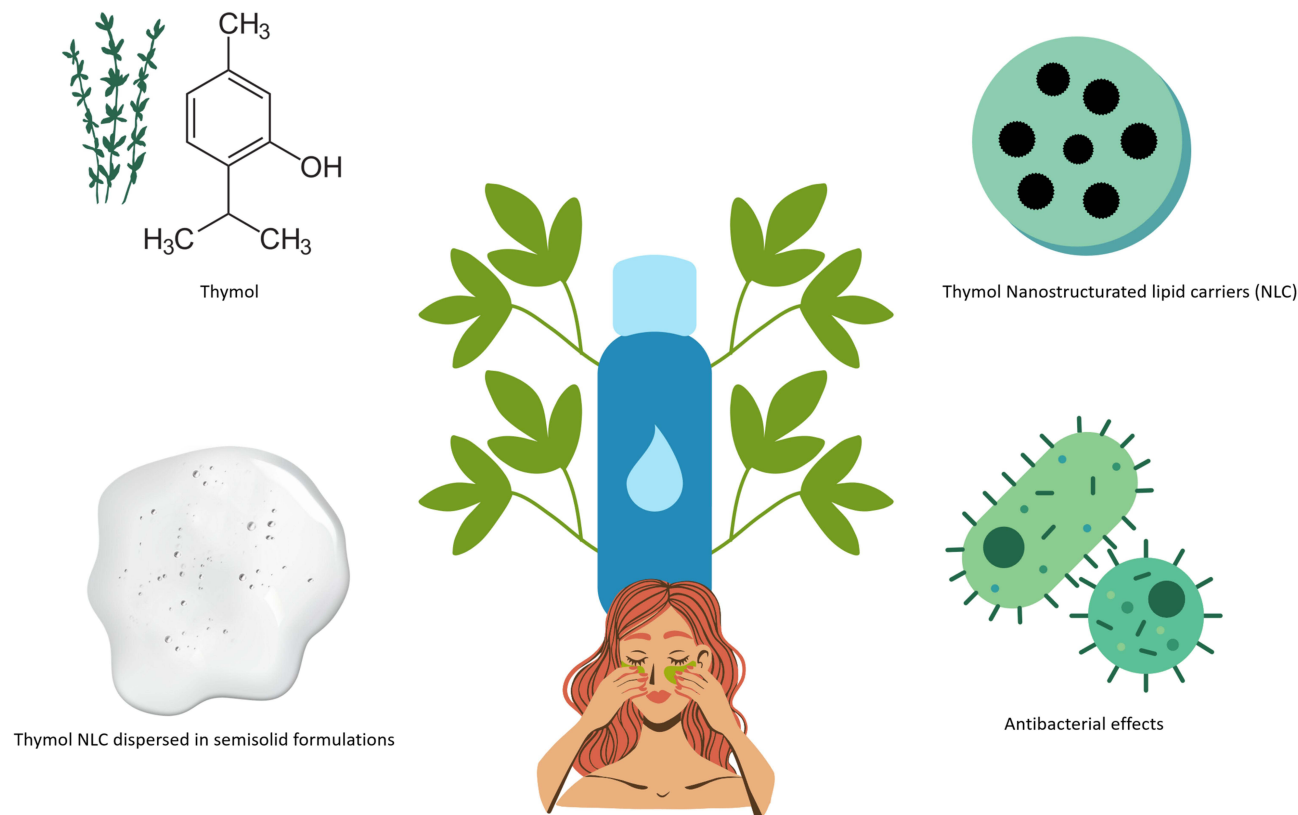
Conclusion: Thymol was successfully loaded into NLC and dispersed in gelling systems, demonstrating that it is a suitable candidate for topical administration against acne vulgaris by eradicating pathogenic bacteria while preserving the healthy skin microbiome.

Keywords: lipid nanoparticles, thymol, acne vulgaris, NLC, gels, antimicrobial

Introduction

Acne vulgaris is one of the most prevalent skin inflammatory disorders affecting approximately 9.5% of the population worldwide.^{1,2} The adolescent affection is highly prevalent and one of the most common dermatoses (between 28.9 and 91.3% of teenagers are affected), and it is concomitant with significant impact on the quality of life.^{3,4} Acne is a multifactorial disease with a complex pathophysiology, in which several internal and external factors are involved, such as irregular keratinocyte proliferation and differentiation, increased sebum production as well and imbalances in the skin microbiota related to *Cutibacterium acnes* (previously known as *Propionibacterium acnes*). In addition, exogenous factors can also trigger acne development.^{5,6} This combination leads to skin lesions such as whiteheads, pustules, and cysts, resulting in swelling and inflammation.⁷

Graphical Abstract



Skin microbiota is an ecosystem composed of several microorganisms (MOs), which are generally non-pathogenic, on the skin surface and internal layers. Their biological function is to protect against external pathogens that can affect the skin and overall health. The *transient microbiota* colonizes the superficial layers of the skin and is likely to be removed by routine hygiene. The *resident microbiota* is consistent with skin survival, mainly found on the surface, under the superficial cells of the stratum corneum (SC). Protective microbiota consists of developing microbial antagonism and nutrient competition for the stability of the dermal ecosystem. Following this strategy, adherence to pathogens was prevented. There is evidence of a relationship between bacteria, skin cells, and immune cells, which reinforces and repairs the skin barrier, improves defense against infection, and diminishes excessive inflammation.⁸ There are two major resident species on the skin: *Staphylococcus epidermidis*, which is the most abundant non-pathogenic bacterium of human skin, that provides a probiotic function by preventing colonization of other pathogenic bacteria,⁹ and *C. acnes* that acts as non-pathogenic balancing the skin microbiota and maintains the acidity and sebum levels of the skin. However, it has been observed that *C. acnes* also proliferates in acne skin, in combination with other factors, leading to mild-to-severe inflammation.

The most common treatment for acne during the past four decades has been the use of an antibiotic drug. However, owing to current antibiotic resistance and the fact that some of these antibiotics possess questionable activity against neutrophil-derived reactive oxygen species (ROS),¹⁰ other strategies are being sought. Moreover, this worldwide increase microbial resistance has been caused mainly by the long-term and frequent use of antibiotics, which has led to a decrease in the skin protective function against infection and inflammation and the unbalanced skin host-microbiome. In this area, natural products are gaining increased attention, since they advocate to be healthier due to their low or non-toxic profile, and therefore, decreased side effects or microbial resistance. Among them, thymol (TH) is of special relevance. TH is a natural compound associated with several activities, such as antioxidant, antimicrobial, antiseptic, and anti-inflammatory.^{11–17} Studies developed by several authors¹⁰ showed the capacity of TH to increase skin elasticity and porosity, which are essential for the healing

process to avoid acne scars. In addition, because bacteria involved in acne are hosted throughout the skin layers, as well as near the follicle, a carrier capable of reaching these sites through a sustained release and permeation rate, delivering the active compound slowly and in a prolonged manner, will be of great relevance.^{7,18}

In this sense, the second generation of lipid nanoparticles, nanostructured lipid carriers (NLC), represent an attractive approach because of their increased stability by reducing drug expulsion, high loading capacity, ability to provide prolonged drug release, improved permeability through skin tissues, and moisturizing properties.^{19,20} These may constitute a suitable alternative to encapsulate lipophilic compounds such as TH and apply them to the skin. Thymol is a monoterpene, a type of molecular structure that is known to act as skin penetration enhancers, by disrupting the lipids of the stratum corneum.²¹ In this sense, the skin permeation of thymol is fast, and therefore, the amount and time retained inside the skin are short. Moreover, TH is an antioxidant molecule, which along storage, may undergo degradation by light, oxygen or humidity, if formulated in its free-form, specially to preserve other antioxidant molecules. For this reason, encapsulating TH would be an advantageous strategy, since it can increase the shelf-life of TH under long-term storage, as well as retained inside the skin. Additionally, NLCs would be promising to improve TH properties inside the skin, since the carriers will act as SC barrier repair, returning the lipids, disrupted by the non-encapsulated TH, to their packed organization, increasing skin hydration. Moreover, the strategy of encapsulating TH into NLC is to develop a nanosystem providing slow-rate release, delivering small dosages inside the skin for a prolonged period, increasing the efficacy of the treatment.

The mechanism of the transdermal permeation of lipid nanoparticles remains unclear. However, previous studies have suggested that the interactions between lipid nanoparticles and skin lipids occur via a dynamic diffusion process.²² Other authors have proposed that the main mechanism of lipid nanoparticles skin penetration is related to their close contact with the stratum corneum (SC) superficial junctions, penetrating the corneocyte bricks.²³ This permits superficial spreading of the active layer, consequently forming an adhesive layer with occlusal properties.²⁴ This would create an antimicrobial protective barrier on the skin surface, avoiding the contact of pathogenic microbes into the affected area, as well as improving the skin barrier regeneration, healing and hydration. This effect may reduce corneocyte packing due to SC hydration, improve drug partitioning, and allow lipid exchange between the nanosystem and the SC. Moreover, if the skin barrier is weakened by skin conditions, such as acne, it increases transepidermal water loss from altered barrier function and may irritate and dry out the skin.²⁵ The decrease in skin barrier hydration and increased transepidermal water loss on skin acne patients have been previously proven.²⁶ Moreover, the same was found for patients treated long-term with either topical retinoids or benzoyl peroxide, unless treated in combination with a moisturizer.⁴ In addition, the correlation of poor skin hydration and enhanced severity of acne lesions have been previously reported.²⁷ In fact, recent studies have shown the potential of lipid nanoparticles to penetrate hair follicles due to the similar composition of the sebum and the lipid nanocarrier,^{28,29} since both may contain triglycerides, diglycerides, wax esters, free fatty acids, and cholesterol.³⁰ For this reason, the combination of occlusive properties of NLCs, the ability to penetrate the skin through the hair follicle and the antimicrobial, antioxidant and anti-inflammatory activity of TH would be promising to treat acne without side effects, loss of skin hydration or microbial resistance.

Therefore, since previous studies by our group showed promising results encapsulating TH into polymeric nanoparticles,³¹ in this manuscript, the optimization of a formulation based on NLC encapsulating TH (TH-NLC) has been carried out. In addition, this formulation was characterized and dispersed into different gelling systems, and its biopharmaceutical parameters and antimicrobial efficacy were assessed and compared. Moreover, therapeutic activity against *Acne vulgaris* and its ability to preserve healthy microbiota have been studied.

Materials and Methods

Materials

Thymol (TH), Tween 20 (TW), poloxamer 188 (P), caprylic/capric triglyceride (Miglyol 812) (CCTG), benzalkonium chloride (BZ), glycerin (GLY), propylene glycol (PG), hydroxypropyl methylcellulose (HPMC), and poloxamer 407 (Pluronic® F127) (PP) were acquired from Sigma-Aldrich (Madrid, Spain). Glyceryl behenate (GBH) (Compritol CG 888 ATO), PEG-8 Caprylic/Capric Glycerides (PCCG), and Transcutol P® (Diethylene glycol monoethyl ether) were provided by Gattefossé (Cedex, France). Carbomer® 934 (Polyacrylic acid, CB) was purchased from Fagron Iberica

(Barcelona, Spain). Double-distilled water was filtered through a Millipore filter (Molsheim, France). All other reagents used were of analytical grade.

DMEM (Dulbecco's Modified Eagle's medium) was purchased from ThermoFisher, MTT (3-(4,5-Dimethylthiazol-2-yl)-2,5-diphenyl tetrazolium bromide) from Sigma-Aldrich (St. Louis, MO, USA) and DMSO (99% dimethyl sulfide) from Sigma-Aldrich (Barcelona, Spain).

Mueller–Hinton broth (MHB), Brain Heart Infusion (BHI), Clostridium reinforced medium (CRM), Tryptone Soy Agar (TSA), and Sabouraud Dextrose Agar (SDA) were purchased from Oxoid (Basingstoke, UK). Beren (cosmetic diluent) was acquired from Scharlab (UK).

Preformulating Studies and Optimization of TH-NLC

Prior to the elaboration of TH-NLC, the compatibility of the mixture of total lipids (solid and liquid proportion) and the amount of TH to be encapsulated was studied. The selected solid lipid (SL) was GBH and the liquid lipids (LLs) were PCCG and CCTG. Briefly, mixtures (SL:LL) were analysed alone (60:40, 70:30, 80:20, and 90:10) as a total lipid portion of 2% or TH-loaded with a total amount of 0.5% TH. The mixtures were performed in test tubes heated in a water bath (80 °C), then using a vortex, and allowed to cool down prior to further analysis.

The compatibility of the mixture of total lipids (solid and liquid proportions) and the amount of TH to be encapsulated were assessed by differential scanning calorimetry (DSC) using a Mettler TA 4000 system (Greifensee, Switzerland).^{32,33} This method is a thermodynamical tool for direct assessment of the heat energy uptake, which occurs in a sample within a regulated increase or decrease in temperature. The difference in the input energy required to match the temperature of the sample, would be the amount of excess heat absorbed (endothermic) or released (exothermic) by the molecule in the sample.³⁴ The DSC measurements were performed, and samples were heated from 5 °C to 100 °C at 10 °C/min under a nitrogen atmosphere. Thermograms were obtained using Mettler STARe V 9.01 DB software (Mettler, Toledo, Spain).^{35,36}

Preparation, Characterization and Optimization of TH-NLC

The production of TH-NLC was developed by two different high-energy procedures, ultrasonication probe (US) and high-pressure homogenization (HPH), using a Sonics Ultrasonic probe (Sonics & Materials Inc., CT, USA) or a high-pressure homogenizer Stansted FPG 12800 (Stansted, United Kingdom), respectively. Briefly, to produce TH-NLC with Tween 20 (TW), both the aqueous phase containing TW as well as the lipid phase containing 0.5% of TH and 2% of total lipid mixture, ranging from 60:40 to 90:10 ratio (SL:LL), were heated above 80 °C. The aqueous phase was added to the lipid phase forming a pre-emulsion using an Ultra-Turrax T25 (IKA, Germany) for 2 min by at 5000 rpm, followed either by US for 20 min at 40% amplitude or by HPH (3 cycles at 700 mbar), and immediately cooled down under cold running water for 5 min.^{36,37} Samples were stored overnight for further characterization.

Samples were optimized by design of experiment (DoE) using a 2²-star factorial design (two levels, two factors, and two central points) developed using the program Statgraphics Centurion XVI.II version 16.2.04 software (Virginia, USA). Based on the previously obtained results, a central point (0) was chosen as function of best values obtained trying both preparation methods, and two independent variable factors (−1/+1) were selected (SL:LL and TW %) to evaluate their influence on TH-NLC properties.³⁶ For this, the concentration of TH was set to 0.5%, the highest dosage reported as safe by the cosmetic ingredients review (CIR).³⁸ The lipid mixtures were 60:40 (−1), 70:30 (0) and 80:20 (+1), and the concentration of TW was 1.2% (−1), 1.6% (0) and 2% (+1). The dependent variables studied were average particle size (Z_{av}), polydispersity index (PI), and encapsulation efficiency (EE).

The physicochemical characterization of TH-NLC (Z_{av} and PI) was performed by dynamic light scattering (DLS) using a ZetaSizer Nano ZS (Malvern Instruments, Malvern, UK). This technique allows to determine the morphometrical properties of the nanoparticles by photon correlation spectroscopy,³⁹ measuring the scattered light intensity dispersion due to the Brownian's motion. The PI is the measure of particle size distribution where values closer to 0.100 and below are considered a monodispersed system.⁴⁰ For these measurements, the samples were previously diluted with Milli-Q water (1:20).

The EE (%) of TH was indirectly measured. Samples were diluted 1:20 in Milli-Q water:ethanol (90:10) and centrifuged (Centrifuge 5415C, Geratebau Eppendorf GmbH, Engelsdorf, Germany) for 10 min at 14,000 rpm using a Millipore filter device (Amicon® Ultra, 0.5 mL 100 K, Merck Millipore Corporation, Massachusetts, USA). The filtered

fractions were quantified by high performance liquid chromatography (HPLC), and EE was determined using Equation (1).

$$EE(\%) = \frac{C_i - C_f}{C_i} \cdot 100 \quad (1)$$

where C_i was the initial concentration of TH and C_f the concentration of the unloaded amount found in the filtered fraction.

Quantitative analysis of TH was performed using reverse-phase HPLC as previously described.³¹ Studies were performed using an Acquity Waters System (Waters 2695) with a UV detector (Waters 2996) (Massachusetts, USA). Briefly, the mobile phase consisted of acetonitrile:water under gradient conditions (30:70, 58:42, 30:70) for 20 min, using a Kromasil[®] column (C_{18} , 5 μ m, 150×4.6 mm, Tecknokroma, Spain). TH was determined at $\lambda_{275\text{nm}}$ and the data were processed using Empower 3[®] software (Waters, Milford, MA, USA).

Preparation of Gels

In this study, three different gelling systems were developed, characterized, and compared for TH-NLC dispersions. For the preparation of the gels, TH-NLC (0.25% or 0.5%) were incorporated at 40% or 50% of the total water content, obtaining a final TH concentration of 0.1% or 0.25%, respectively. For free TH gels, TH was previously dissolved in 5–10% of glycerin or propylene glycol under continuous vigorous stirring, then added to the water phase the equivalent concentration (0.1% or 0.25% TH). Carbomer gels (GC-TH-NLCs) were formulated by previously dissolving Carbopol 0.5–1% in water under constant magnetic stirring and then adding 5% of glycerin or propylene glycol. The mixture was then allowed to stand overnight, and the pH was adjusted to 5.0–6.5 with NaOH 2N. For the hydroxypropyl methylcellulose (HPMC) gels (GH-TH-NLCs), HPMC was dissolved in the water phase (2–5%), and 5% of glycerin or propylene glycol (5%) were added. For the Pluronic gels (GP-TH-NLCs), P407 (20%) was dissolved in cold water under continuous stirring. Then, the mixture was allowed to stand overnight at 4 °C and glycerin or propylene glycol (5%) were added and mixed under vigorous stirring. The gel was formed at room temperature (RT). All gel mixtures were emulsified using an Unguator[®] (Microcaya, Bilbao, Spain).

Characterization of TH-NLC and TH-NLC Gels

The morphology of TH-NLC was determined by transmission electron microscopy (TEM) JEOL 1010 (Tokyo, Japan). The formulation was negatively stained with 2% uranyl acetate and added to a copper grid coated with carbon film. The samples were dried overnight in a desiccator at room temperature.³¹ Images were obtained using MegaView III software (Soft Imaging Systems, GmbH, Münster, Germany).

Scanning electron microscopy (SEM; JSM-7001F, JEOL, Tokyo, Japan) was used to assess the morphology of TH-NLC gels. The solid sample was coated with a carbon layer or thin metal layer and deposited on a metal support for subsequent sputtering copper coating for analysis.⁴¹ The samples of GC-TH-NLC were dehydrated by incubation (30 °C) for 5 days.

Short-Term Stability

The short-term physical stability of the developed formulations was studied using an optical analyzer (Turbiscan[®] Lab Expert; Iesmat, Madrid, Spain) based on the analysis of multiple light scattering to identify any destabilization phenomena of the colloidal suspension. The method is based on the variation of the droplet volume fraction (migration) or the diameter (coalescence) that results in a variation of the scattered or transmitted lights.⁴² A glass measurement cell containing approximately 20 mL or 20 g of sample was used, and a light source corresponding to pulsed near-infrared light was applied. The backscattering (BS) signal was measured using a detector at an angle of 45° from the incident beam.⁴⁰

Selected samples were evaluated during storage at room temperature (RT) for up to six months by measuring the pH and observing the organoleptic properties (appearance, colour, and odour).

The microbial preservative stability of GC-TH and GC-TH-NLCs was evaluated after storage at RT for 6 months using the plate inclusion technique. For this, 100 mg of gel was transferred onto TSA or SDA plates for bacteria, fungi, or yeast. The total microbial viable count was determined after incubation at 35 ± 2 °C for 3 days or at 28 ± 2 °C for 7

days, respectively. This method was developed based on the specifications of the European Pharmacopeia monograph (2.6.12. Microbiological examination of non-sterile products: total viable aerobic count) as previously described.³¹

Rheology Studies of TH-NLC Gels

Rheological measurements study the viscosity of the system and the fluid behaviour according to the shear force used, where formulations are subjected to variable controlled deformations measuring the stress. This assay was performed using a Haake Rheostress[®] 1 rheometer (Thermo Fisher Scientific, Karlsruhe, Germany) connected to a thermostatic circulator (Thermo Haake Phoenix II + Haake C25P) and a computer Pc provided with the Haake RheoWin[®] Job Manager and Data Manager software v. 4.91. The measurements were performed in rotational mode with a cone-and-plate geometry (C60/2°Ti: 60 mm diameter, 2° angle). The shear stress (τ) was measured as a function of the shear rate ($\dot{\gamma}$). Viscosity curves ($\eta = f(\dot{\gamma})$) and flow curves ($\tau = f(\dot{\gamma})$) were recorded at $25 \pm 0.1^\circ\text{C}$. The shear rate ramp program included a 3 min ramp-up period from 1 to 100 s^{-1} , a 1 min constant shear rate period at 100 s^{-1} , and a 3 min ramp-down from 100 to 1 s^{-1} . The data from the flow curves were fitted using mathematical models to identify the model that provided the best overall match with the experimentally observed rheological data. The adequacy of the rheological profiles for the mathematical models was based on the correlation coefficient (r) and the chi-square values. The viscosity (η , Pas) was determined from the constant shear section at 100 s^{-1} .⁴³

In vitro Drug Release

The biopharmaceutical behaviour of the aqueous formulations (TH and TH-NLC) and their respective gelling systems was evaluated using the same method as previously described.³¹ The study was carried out using vertical diffusion Franz cells (FDC-400, Crown Glass, NJ, USA) with a thermal bath set to 32°C , to mimic skin in vivo conditions, under constant stirring. For this study, methylcellulose membranes (Dialysis Tubing Visking, MW 12.000–14.000 Da, London, UK) were placed between the donor and receptor compartments (2.54 cm^2). The receptor phase was filled with Diethylene glycol monoethyl ether: water (50:50) to maintain the sink conditions. Samples ($300 \mu\text{L}$) were collected at selected times (3, 8, 12, 20, 24, 28, 34, 40, 48, 64, 72 min), and replaced with the same volume of receptor medium.⁴⁴ Data were analysed using HPLC (as described previously), and the results were processed using GraphPad. Variable mathematical models were applied to determine the best-fit kinetic profile: zero order, first order, hyperbole, Higuchi, Korsmeyer Peppas, and Boltzmann Sigmoidal.⁴⁵ Statistical analysis was performed using one-way ANOVA and Tukey's multiple comparison test.

Ex vivo Skin Permeation Studies

Ex vivo permeation experiments were performed using human skin explants obtained from the plastic surgery of the abdominal region of a healthy female (Barcelona-SCIAS Hospital, Barcelona, Spain) and were performed in accordance with the Declaration of Helsinki. The donors provided written informed consent and the experimental protocol was approved by the Research Commission of Barcelona SCIAS Hospital (Barcelona, Spain).^{46,47} The experimental procedure and quantitative analysis of TH were carried out according to a previously described method, with modifications.^{31,48} This study consisted of three experiments set up to find comparable analysis and they were all performed in Franz cells using the same conditions described above. Skin samples (0.64 or 2.54 cm^2 , 0.4 or 1 mm thick) were placed with the SC facing up, and the donor compartment was filled with TH, TH-NLC, or their gel formulations (at 0.25% of TH). The amount of TH penetrating the skin at selected times (4, 8, 12, 15, 18, 20, 24 h), at 32°C , was measured by HPLC, and data were analysed using GraphPad Prism. Statistical analysis was performed using one-way ANOVA Tukey's multiple comparison test, or unpaired t -test. The skin permeation parameters were calculated using Equation (2):

$$J = K_p \cdot C_0 \quad (2)$$

where J is the flux, K_p is the permeability coefficient, and C_0 the initial active-component concentration.²⁰

To determine the total amount retained inside the skin (Q_s), samples were cut, weighed, perforated with needles, 1 or 2 mL of ethanol: water (50:50) were added and kept in an ultrasonic bath for 20 min.⁴⁹ The amount of TH extracted was determined using HPLC and calculated using a previously obtained recovery factor.³¹

Another experiment was conducted to evaluate the skin penetration of the TH-NLC using SEM. Fresh ex vivo skin explants were obtained and the fat tissue was immediately removed with sterile surgical razors. Skin samples were cut and placed on Franz cells (0.64 cm²) using PBS as the receptor medium. GC-TH-NLCs were applied to the skin and incubation was performed for 24 h at 32 °C. Thus, skin samples were washed and cut into small pieces, fixed for 2 h with 4% paraformaldehyde and 2.5% glutaraldehyde in 0.1 M sodium cacodylate buffer (pH 7.4), post-fixed with 1% osmium tetroxide for 2 h at 4 °C, and stained in 0.5% uranyl acetate for 45 min at 4 °C. After dehydration with alcohol gradients, the samples were dried at the critical point (Emitech K850) and mounted on a conductive adhesive disc (carbon tabs, Agar Scientific), followed by carbon coating under evaporation (Emitech 950). The images were analyzed using SEM (Jeol JSM-7001F).⁵⁰

Cell Viability Assay

The cytotoxicity of TH-NLCs was determined by the viability of human epidermal keratinocyte cell lines (HaCaT, spontaneously immortalized human keratinocytes, Addexbio catalog %:T0020001) at several concentrations, as previously described elsewhere.³¹ In the case of washed particles (-w), they were washed three times to remove excess TW (centrifugation at 14,000 rpm for 15 min). Briefly, HaCaT cells were cultured in high glucose supplemented DMEM (10% foetal bovine serum (FBS), 2 mM l-glutamine, 100 units/mL penicillin G, and 100 µL/mL streptomycin). The cells were adjusted to a density of 2×10^5 cells/well using an automated cell counter (Invitrogen Countess, ThermoFisher) and seeded (100 µL) in 96-well plates. Diluted samples were added and incubated for 24 h at 37°C and 5% CO₂. Then, MTT (0.25%) was added to determine the cell viability. After 2 h of incubation, the medium was replaced with 100 µL DMSO.⁵¹ Cell viability was measured at $\lambda_{570 \text{ nm}}$ using a Modulus Microplate Photometer (Turner BioSystems Inc., Sunnyvale, CA, USA). Results were expressed as the percentage of cell survival relative to untreated cells, and statistical analysis was performed by *t*-test, comparing each concentration used.

In vitro Antimicrobial Efficacy

The antimicrobial activities of TH and TH-NLC were studied as previously described,³¹ using an inoculum of *Cutibacterium acnes* (*C. acnes*) or *Staphylococcus epidermidis* (*S. epidermidis*). *C. acnes* was cultured in BHI medium for 48 h at 37 °C under anaerobic conditions, using parches AnaeroGen[®] and indicator (Oxoid, Basingstoke, UK). *S. epidermidis* was cultured in MHB medium for 24 h at 37 °C. Prior to each experiment, each inoculum was prepared in PBS adjusted to 0.5 MacFarland (McF) standard to obtain 1.5×10^8 colony forming units/mL (CFU/mL). Microbial counts were performed on CRM or TSA plates.

The minimal inhibitory concentrations (MIC) of TH and TH-NLC were determined using the broth microdilution assay.⁵² Briefly, double-concentrated sample dilutions were prepared and added (100 µL) to a double-concentrated culture medium (100 µL) in a 96-well polypropylene microtiter plate (Costar, Corning Incorporated, Corning, USA). Then, *S. epidermidis* (10 µL) or *C. acnes* (20 µL) was added to inoculate wells at final TH concentrations from 2 to 1024 µg/mL or 2 to 1000 µg/mL, followed by incubation at 37 °C for 24 or 48 h, respectively. Additionally, the minimal bactericidal concentration (MBC) was determined by transferring 10 µL of each sample without *C. acnes* into BHI agar plates, followed by further incubation. Positive and negative growth controls were used.³¹

The decimal reduction time assay (D) was used to determine the reduction in bacterial viability at determined contact times⁵³ using TH or TH-NLC and their carbomer gels (GC-TH and GC-TH-NLCs), using the same method as previously described.³¹ Inoculum of *C. acnes* or *S. epidermidis* was prepared in PBS (10^8 CFU/mL) and added (100 µL) to each experimental test tube (10 mL) containing several dilutions of TH or TH-NLC. For *C. acnes*, the formulations were diluted with water (250, 500, and 1000 µg/mL), corresponding to the MIC, 2X MIC and 4X MIC, respectively. The gel was assessed at a concentration of 1000 µg/mL. For *S. epidermidis*, formulations (aqueous and gel) were used at 1000 µg/mL, representing 2X MIC. Tubes were incubated at 32 °C for predetermined times, and samples were neutralized (1:10) in Beren's diluent for 15 min. They were subsequently diluted in PBS and microbial counts were performed on

CRM or TSA agar plates. Bacterial viability was expressed as log CFU versus time (h). The decimal reduction time (D), which is the time taken to reduce the decimal value to the initial value, was determined by calculating the inverse of the slope (1/b). Statistical analysis was performed using one-way ANOVA, Tukey's multiple comparison test, and an unpaired *t*-test.

Ex vivo Antimicrobial Activity

Bacterial viability was evaluated in human skin explants obtained from abdominal plastic surgery (Hospital de Barcelona, SCIAS, Barcelona, Spain), based on previous studies and in accordance with the Declaration of Helsinki.^{31,54} Briefly, skin samples (0.6 cm²) were placed into petri dishes with the SC on the top adding PBS-wet sterile filter paper to keep dermis moisture. A fresh overnight culture of *C. acnes* was prepared in PBS (1.5×10^8 CFU/mL), and skin samples were inoculated with 10 μ L. To study the prevention of the antimicrobial activity, TH or TH-NLC (30 μ L) were applied to the skin surface and incubated at 32 °C for 8 h. Subsequently, *C. acnes* (30 μ L) was inoculated and incubated for 16 h. To study the treatment capacity, *C. acnes* (30 μ L) was first applied to the skin for 30 min and then treated with products for 24 h. For both experiments, PBS was used as the control. Skin samples were neutralized in Beren's diluent (1 mL) for 15 min, extracted under sonication for 10 min, then further 10-fold diluted. Microbial counts were performed the spread count method (100 μ L of each sample) in CRM agar plates, incubated under anaerobic at 37 °C for 48 h. To study the dose-dependent antimicrobial activity, *C. acnes* (10 μ L) was applied to the skin. After 30 min, 30 μ L of TH or TH-NLC was applied as a single or multiple dose (1, 2, or 3) at predetermined timepoints (0, 12, and 18 h) and incubated at 32 °C. After 24 h, neutralization and sample dilution were performed, as described above. The microbial count was determined using the drop count method (10 μ L) on CRM agar plates. Viable bacterial counts were expressed as log/CFU per treated skin. Statistical analysis was performed using one-way ANOVA, Tukey's multiple comparison test, and an unpaired *t*-test.

Results

Preformulation Experiments

The selection of NLC lipid components and their ratios was optimized by means of their thermal interactions, and the results are shown in Figure 1. SL was GBH because of its excellent skin emollient and smoothing properties.⁵⁵ A screening of several combinations of GBH with two different LL was carried out. Therefore, PCCG and CCTG were studied.

In the case of PCCG, it can be observed that in the lipid mixtures without TH (blank mixtures) (Figure 1A), different ratios of lipids did not alter the melting point of the lipid structure, presenting values around 70 ± 0.9 °C. However, after adding TH at 0.5% (Figure 1B), the melting point of the mixtures was slightly decreased to 69 ± 0.5 °C. In addition, no melting point modifications were observed at other ratios (60:40 to 90:10).

In the case of CCTG, it can be observed that the blank mixture provided melting point values ranging from 67 to 71 °C (Figure 1C), and by adding TH, these values also decreased up to 64 to 69 °C (Figure 1D). Additionally, for both combinations of lipids, the incorporation of TH was suitably blended because no peaks of TH were observed at 51 °C in the lipid mixture thermograms. Therefore, both liquid lipids were suitable for the development of TH NLC. Despite this, PCCG exhibited less variation in the NLC melting point, and TH exhibited better solubility in PCCG than in CCTG; therefore, PCCG was chosen as the liquid lipid. Moreover, the different SL:LL ratios showed different textures, being thicker at higher ratios (soft at 60:40, medium-soft at 70:30, and hard at 80:20).

Optimization by Design of Experiments

Prior to development of DoE, an optimization process was carried out by preparing NLC using HPH and US, to establish the most suitable method for producing TH-NLC evaluating the physicochemical parameters. Therefore, increasing ratios of solid and liquid lipids and two concentrations of TW were used. The combination of these parameters was analyzed using Z_{av} and PI. The results obtained by TH-NLC comparing both preparation methods showed that the Z_{av} of the TH-NLC obtained using HPH was smaller (Table 1). To obtain Z_{av} suitable for skin applications, NLC values between 200 and 400 nm were obtained.⁵⁶ The most suitable results were obtained using a lipid mixture of 70:30, which also

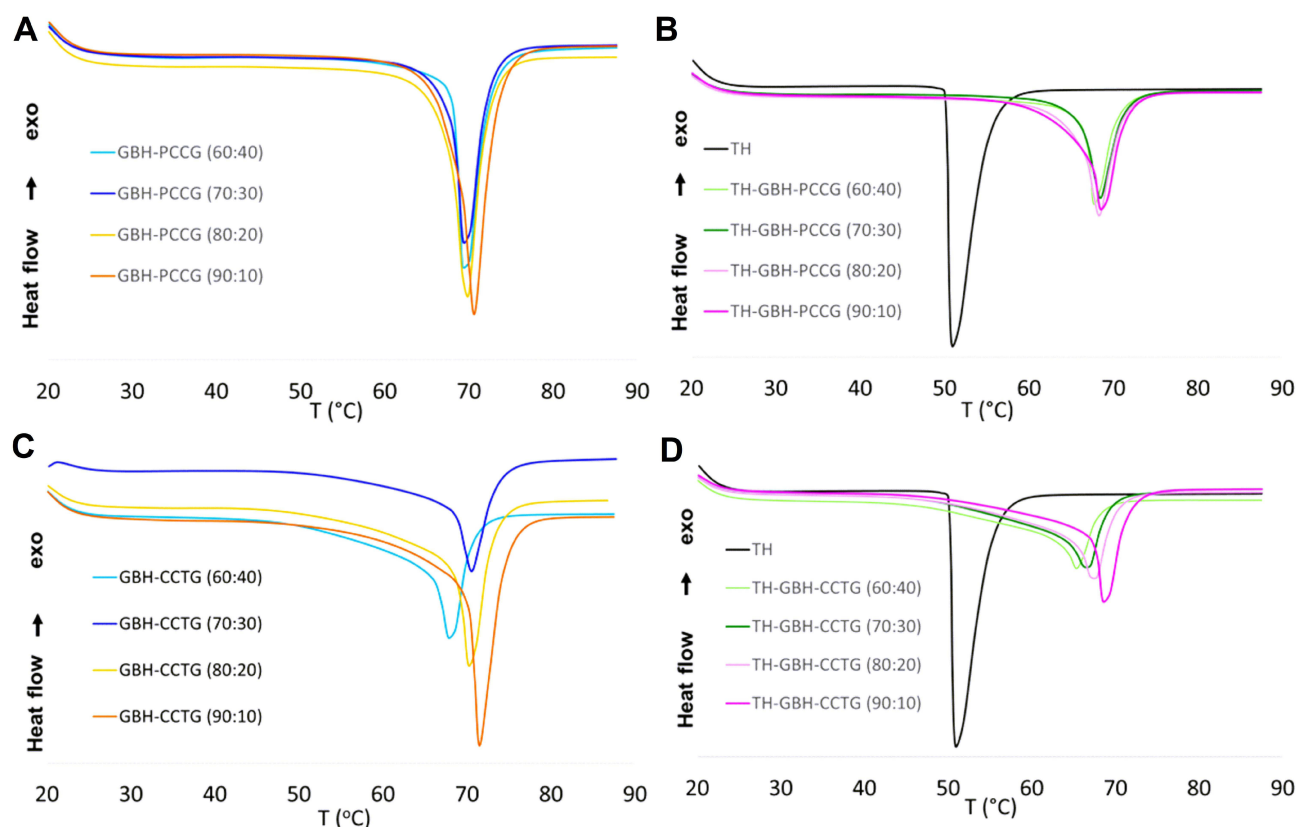


Figure 1 DSC thermograms of lipid mixtures using the solid lipid with two different liquid lipids, with or without thymol: (A) GBH-PCCG, (B) GBH-PCCG-TH, (C) GBH-CCTG and (D) GBH-CCTG-TH.

corresponded to a medium-soft texture. In the case of the other SL:LL proportions, 60:40 texture was found slightly soft, while 90:10 presented a hard structure and lower solubility of TH in the LL. The solubility of TH in the LL is important to maintain the advantages of the NLC towards solid lipid nanoparticles (SLN), since the latter possess diminished loading capacity and Th may suffer from a crystallization process being expelled from the lipidic carrier. Therefore, the selection of the SL:LL proportion was considered to obtain the highest amount of TH encapsulated. Moreover, the comparison of the physicochemical parameters (Z_{av} and PI) was based on obtaining suitable size for skin application,

Table 1 Comparative Physicochemical Characterization of TH-NLC Produced with Two Variable Factors (Lipid Proportion and Surfactant Concentration) and Two Variable Preparation Methods (HPH and US)

GBH:PCCG	TW (%)	High Pressure Homogenization		Ultrasound	
		$Z_{av} \pm SD$	$PI \pm SD$	$Z_{av} \pm SD$	$PI \pm SD$
90:10	I	173.6 \pm 2.2	0.227 \pm 0.021	301.7 \pm 2.1	0.259 \pm 0.013
80:20	I	176.6 \pm 3.3	0.280 \pm 0.030	206.0 \pm 4.5	0.218 \pm 0.027
70:30	I	156.9 \pm 3.7	0.192 \pm 0.010	246.7 \pm 5.5	0.189 \pm 0.030
60:40	I	217.8 \pm 5.1	0.175 \pm 0.029	298.8 \pm 32.2	0.359 \pm 0.045
90:10	1.6	123.8 \pm 3.0	0.139 \pm 0.021	326.8 \pm 4.9	0.271 \pm 0.007
80:20	1.6	197.4 \pm 3.9	0.113 \pm 0.039	265.1 \pm 6.4	0.181 \pm 0.022
70:30	1.6	218.4 \pm 3.4	0.135 \pm 0.018	250.9 \pm 2.9	0.139 \pm 0.023
60:40	1.6	263.7 \pm 0.7	0.186 \pm 0.016	360.0 \pm 17.9	0.223 \pm 0.020

Notes: Bold formulation corresponds to the formulation used for the following factorial design.

Abbreviations: GBH, Glyceryl behenate; PCCG, PEG-8 Caprylic/Capric Glycerides; Z_{av} , average size; PI, polydispersity index.

where the range of particle size should be higher than 200 nm, in contrast to others route of administration. In addition to small particle diameter, a monodispersed system should also be accomplished since a monomodal population will be obtained as long as PI values remain around 0.1. For this reason, we found that the values obtained for 70:30 (SL:LL) and 1.6% TW possess low PI and both obtention methods showed similar characteristics.

Based on the obtained results and following the DoE, a central factorial design with two levels and two factors was conducted and US was the selected method to prepare the formulations. The central points of the design corresponded to the formulation with the best physicochemical parameters (Table 1), and a design space was established. The amount of TH was set to a fixed concentration (0.5%), corresponding to the highest dosage described as safe in the Cosmetics Ingredients Review (CIR). Therefore, we aimed to find suitable ratios of lipid mixtures and surfactant concentrations to stabilize the NLC obtaining maximum therapeutic efficacy. The results obtained by analyzing the dependent variables Z_{av} , PI, and EE are shown in Table 2, and the surface responses of the DoE are shown in Figure 2A–C, respectively. Despite the fact that no statistically significant differences were obtained (Figure 2D and Figure S1 of Supporting Information), for a Z_{av} of approximately 200 nm and PI corresponding to homogeneous systems, an intermediate amount of TW as well as ratios of GBH:PCCG of approximately 70:30 should be obtained. According to the surface response plotted, using these intermediate concentrations, EE of more than 80% will be obtained. Therefore, optimized TH-NLC contained 1.6% TW and ratio of GBH:PCCG of 70:30, with Z_{av} below 300 nm, PI corresponding to monomodal systems, and EE values of more than 80%.

Rheological Studies

To design a suitable vehicle to disperse TH-NLCs on the skin and increase TH-NLC therapeutic efficacy, three gel formulations were developed and characterized. The aim of this study was to evaluate the rheological flow of an excipient containing free TH vs TH-NLCs, as well as comparing different types of vehicles for TH-NLCs, based on different gelling materials and increased viscosities. The rheological flow and viscosity of GC, GH, and GP were studied by dispersing thymol (A) GC-TH, (B) GH-TH, (C) GP-TH, or dispersing NLC, (D) GC-TH-NLCs, (E) GH-TH-NLCs, and (F) GP-TH-NLCs. The results obtained are analyzed and are shown in Figure 3. Rheological measurements showed that the formulations were dependent on the shear rate. All formulations exhibited non-Newtonian behavior, with a consistent decrease in viscosity with increasing of shear rate from 1 to 100 s^{-1} . The mathematical model that best fitted the experimental data is Cross equation (3) for the GC and GH formulations, which provides a general model for shear thinning materials (pseudoplastic). For the GP formulations, the best fit is the Herschel-Bulkley equation (4), which characterizes plastic materials. These findings could also be confirmed by the appearance and texture of the gels, where

Table 2 DoE with Two Levels and Two Factors with Two Central Points

Levels		Independent Factors		Response Factors		
SL:LL	TW	SL:LL (%)	TW (%)	$Z_{av} \pm SD$ (nm)	$PI \pm SD$	$EE \pm SD$ (%)
–I	–I	60:40	1.2	361.3 \pm 34.1	0.213 \pm 0.017	81.26 \pm 0.09
–I	0	60:40	1.6	350.6 \pm 20.1	0.202 \pm 0.003	76.98 \pm 1.98
–I	+I	60:40	2.0	327.3 \pm 45.1	0.215 \pm 0.052	77.82 \pm 1.71
+I	–I	80:20	1.2	236.5 \pm 21.4	0.288 \pm 0.048	76.38 \pm 0.15
+I	0	80:20	1.6	286.5 \pm 50.9	0.272 \pm 0.035	76.53 \pm 0.35
+I	+I	80:20	2.0	244.3 \pm 21.1	0.216 \pm 0.048	79.06 \pm 1.59
0	–I	70:30	1.2	351.8 \pm 29.5	0.266 \pm 0.031	77.33 \pm 1.21
0	+I	70:30	2.0	238.6 \pm 5.3	0.218 \pm 0.013	76.96 \pm 1.36
0	0	70:30	1.6	259.3 \pm 29.4	0.119 \pm 0.031	80.42 \pm 1.40
0	0	70:30	1.6	280.0 \pm 23.5	0.121 \pm 0.042	81.41 \pm 0.62

Notes: Responses of physicochemical characterization of TH-NLC produced by two variable factors (lipid proportion and surfactant concentration) using ultrasound are shown as Z_{av} (average size), PI (polydispersity index) and EE (entrapment efficiency) % achieved. SL indicates solid lipid and TW indicates tween 20. Bold values indicate the optimized formulation.

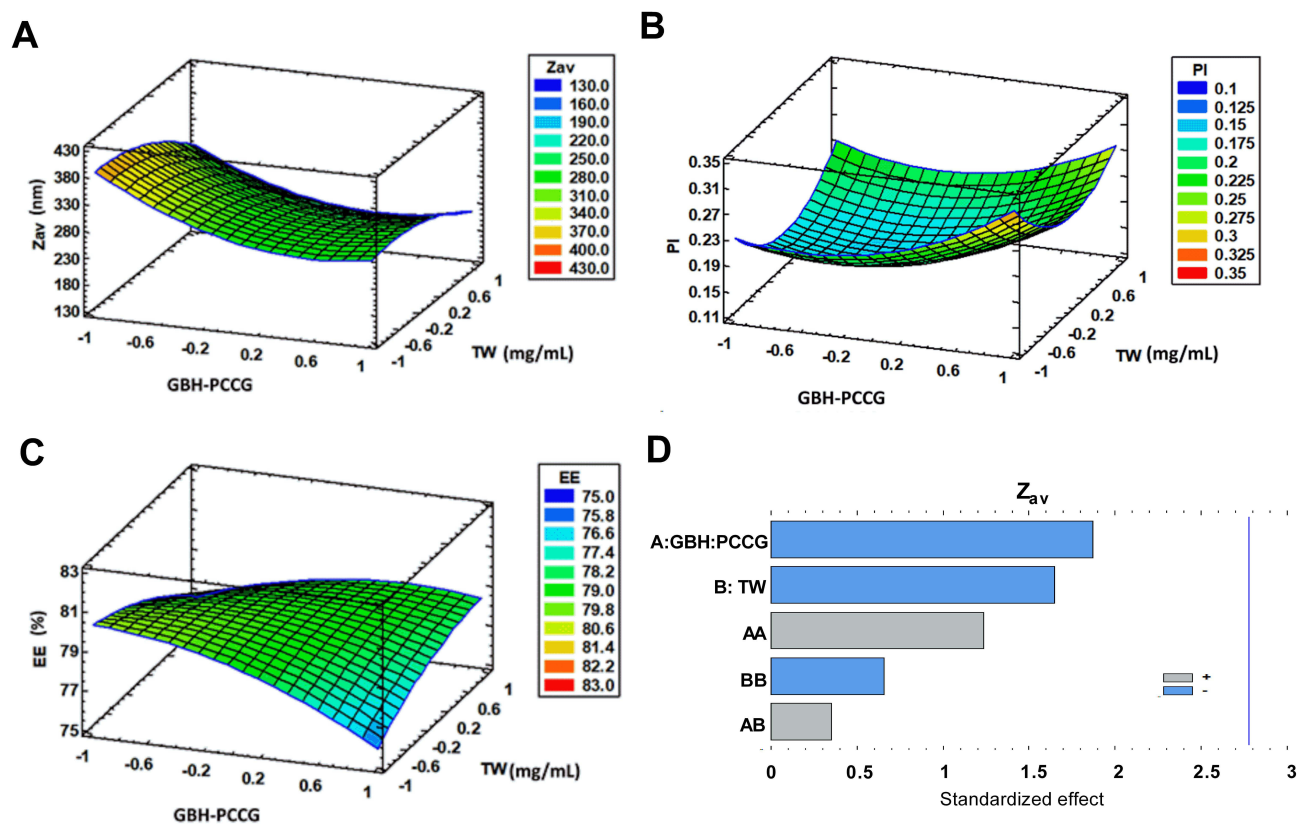


Figure 2 Surface response of TH-NLC by DoE using TH 0.5% plotted for (A) Z_{av} (nm), (B) PI and (C) EE (%). (D) Pareto's chart of Z_{av} .

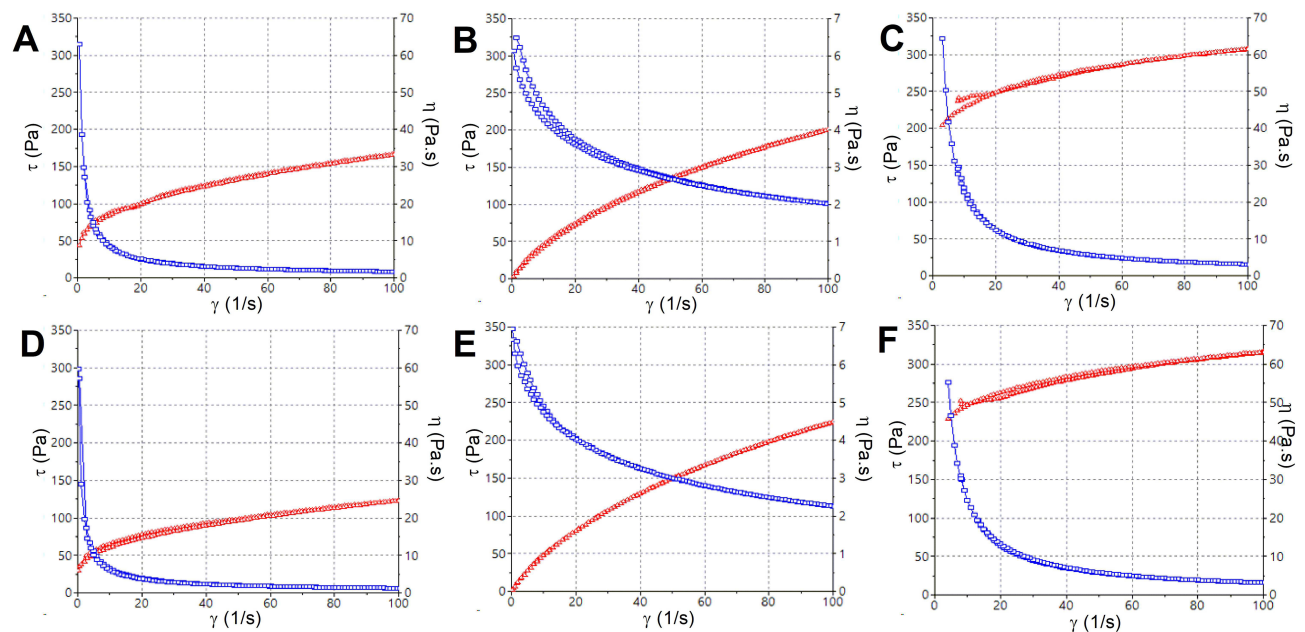


Figure 3 Rheograms of gel formulations of thymol (A) GC-TH, (B) GH-TH and (C) GP-TH, or optimized thymol-NLCs (D) GC-TH-NLC, (E) GH-TH-NLC and (F) GP-TH-NLC. Data was adjusted to Cross (A, B, D and E) and Herschel-Bulkley (C-F) mathematical models, corresponding to a pseudoplastic or plastic flux, respectively.

GCs and GHs provided an easy spreading application onto the skin and, in contrast, GPs showed a more dried touch and non-easy spreadable application. The viscosity of each formulation was determined as $100 \text{ s}^{-1} (\text{Pa} \cdot \text{s})$, as shown in Table 3.

Table 3 Rheology of TH-NLC Gel Formulations

Sample	Viscosity (Pa.s)	Flow	Math Model
GC-TH	1.57 ± 0.00	Pseudoplastic	Cross
GC-TH-NLC	1.23 ± 0.00	Pseudoplastic	Cross
GH-TH	2.01 ± 0.00	Pseudoplastic	Cross
GH-TH-NLC	2.25 ± 0.00	Pseudoplastic	Cross
GP-TH	3.08 ± 0.00	Plastic	Herschel-Bulkley
GP-TH-NLC	3.16 ± 0.00	Plastic	Herschel-Bulkley

Notes: GC-TH indicates thymol dispersed in a carbomer gel, GH indicates thymol dispersed in a hydroxypropyl methylcellulose gel, GC-TH-NLC indicates thymol loaded nanostructured lipid carriers dispersed in a carbomer gel and GH-TH-NLC indicates thymol loaded nanostructured lipid carriers dispersed in a hydroxypropyl methylcellulose gel.

$$\eta = \frac{\eta^0 - \eta^\infty}{(\tau)^m} \quad (3)$$

Where η is the apparent viscosity, η^0 and η^∞ are asymptotic values of viscosity at very low and high shear rate, respectively, τ is the shear stress (Pa), γ is shear rate (1/s) and m is the flow index.

$$\eta = \frac{\tau_0}{y + K * y^{(N-1)}} \quad (4)$$

Where η is the apparent viscosity, τ_0 is the shear stress (Pa) when deformation velocity tends to zero, y is the deformation velocity, K consistency coefficient and N is the flow behavior index.

Morphology Observation by Transmission Electron Microscopy

In addition to the measurements carried out by dynamic light scattering, TH-NLC were analyzed by TEM, confirming that the NLC droplets had a semi-spherical soft shape (Figure 4A), which is characteristic of this type of nanocarrier.³⁶ Moreover, SEM was used to analyze GC-TH-NLC (the carbomer gel containing TH-NLC). The gel matrix structure is shown in Figure 4B and a closer image (Figure 4C). It can be observed that the gel threads have a lipidic texture/appearance, around 1 μ m diameter, where the NLCs were found embedded within. It presented an amorphous lipidic (waxy-like) appearance, similar to an emulgel (non-grease, easy spreadability and easy removable).⁵⁷

Stability of TH-NLC Formulations

Short-term stability was predicted by analyzing the BS profile of TH-NLC and TH-NLC dispersed into the gelling systems, measured by the Turbiscan[®]Lab (Figure 5). This technique allows us to evaluate the NLC stability in solution and the manner the gelling systems stabilize them. The scan runs from bottom-to-top of the vial measuring BS, evaluating the trends of

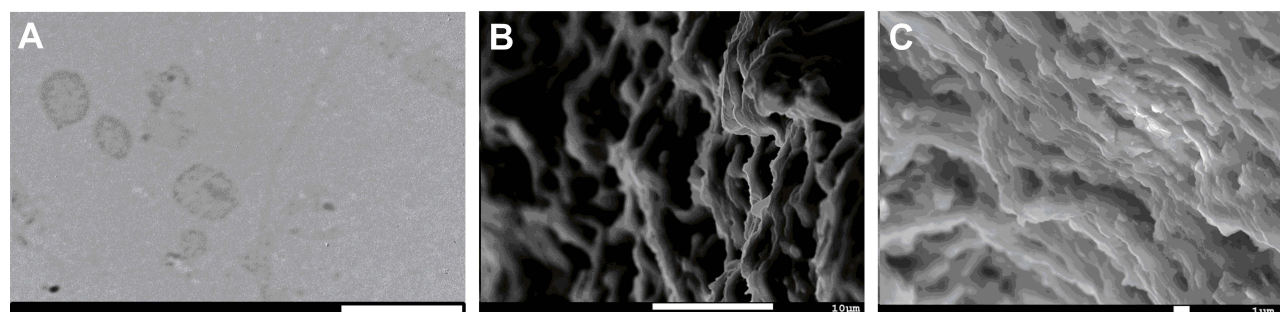


Figure 4 Micrographs obtained by different techniques: (A) TEM of TH-NLC (scale bar 500 nm), (B) SEM image of TH-NLC incorporated into carbomer gel (GC-TH-NLC, scale bar 10 μ m) and (C) SEM image of GC-TH-NLC (scale bar 1 μ m).

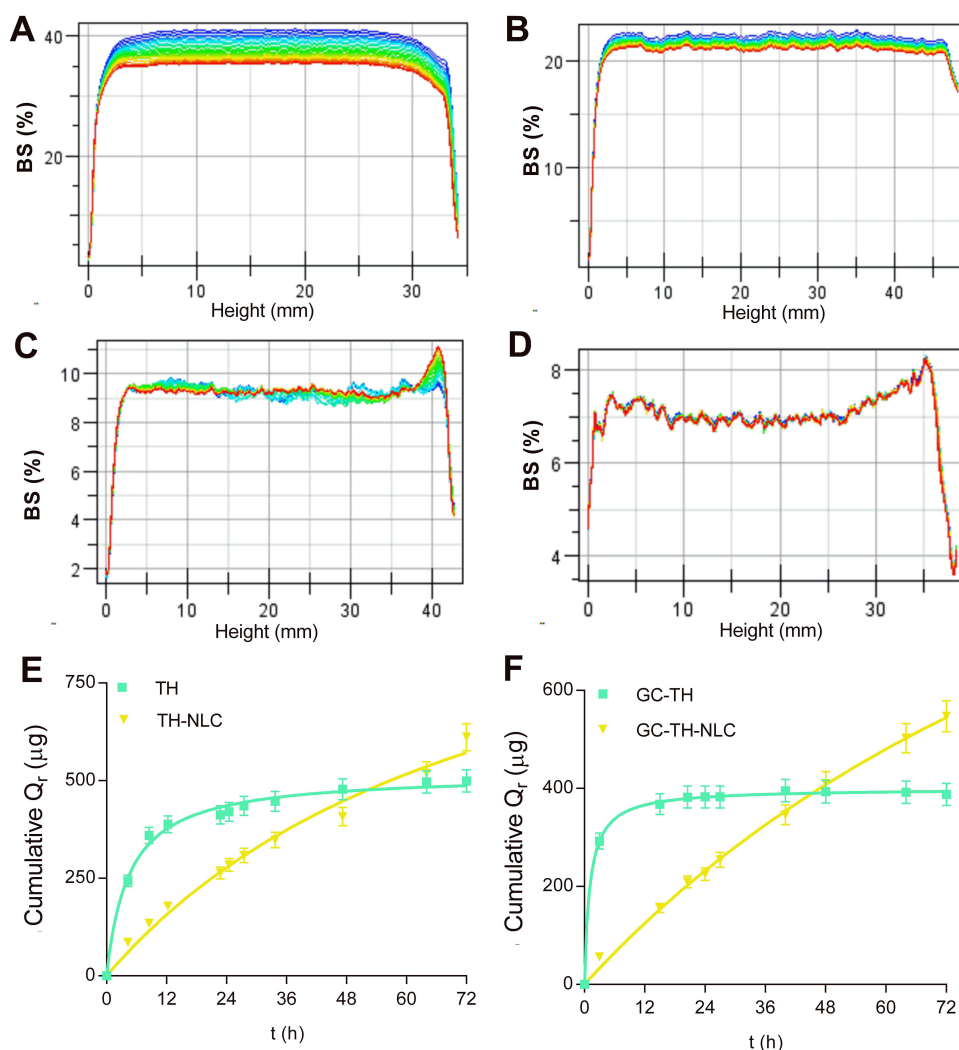


Figure 5 Short-term stability of TH-NLC (A), analyzed by the backscattering signal and those incorporated into variable gel formulations: (B) GC-TH-NLC, (C) GH-TH-NLC and (D) GP-TH-NLC. Scans were performed from the bottom to the top of the vial, measured every hour for 24 h, represented from blue to red lines. In vitro release profile of (E) TH and TH-NLC and (F) GC-TH and GC-TH-NLC, plotted as cumulative amount released (Q_s) adjusted to hyperbole mathematic model.

possible sedimentation, aggregation, flocculation, or creaming. The results showed that TH-NLC, as aqueous suspensions during storage, might lead to flocculation (Figure 5A). However, when these particles were incorporated into gel formulations (Figure 5B–5D) (GC-TH-NLC, GH-TH-NLC, and GP-TH-NLC, respectively), the TH-NLC particles were stabilized, making them suitable for storage to avoid creaming or flocculation phenomena. The BS of TH-NLC and GC-TH-NLCs was also measured after 1-month storage at $4 \pm 2^\circ\text{C}$ and $23 \pm 2^\circ\text{C}$, respectively (Figure S2). Furthermore, the pH of the gel formulations was measured for 6 months at room temperature (RT) ($23 \pm 2^\circ\text{C}$) (information can be found in Table S1), remaining stable, and no color, odor, or appearance variations were observed.

The microbial preservative stability studied for GC-TH-NLCs showed no microbial growth after 6 months of storage at RT, as evaluated for bacteria, fungi, and yeast. Therefore, the antimicrobial activity of thymol exhibited good microbial preservative activity for the carbomer gel during storage, confirming the sterility of the samples throughout the experiments.

In vitro Release of TH-NLC Formulations

The TH release profile was evaluated for 72 h and adjusted to a hyperbola equation (best fit). In Figure 5 (E-F), it can be observed that a sustained release of TH-NLC was found either in the aqueous or gel forms, compared to TH. In both cases, the steady state of non-particulate TH was reached before 12 h, whereas TH-NLC and GC-TH-NLCs provided

prolonged release for 72 h. Statistical analysis showed significant differences in TH-NLC in both aqueous and gel forms at 24 h (Table 4). These findings provide a potential skin treatment using TH-NLCs, since the release inside the skin layers would be prolonged and continuous, and therefore, enhancing the release of TH inside the skin, requiring less dosages and applications.

Ex vivo Skin Permeation of TH-NLC

Skin penetration of TH and TH-NLC was evaluated in human abdominal skin explants using variable dosage forms. First, the three gel formulations with dispersed TH-NLC were compared (Table 5 and Figure 6). The results showed that, depending on the vehicle used, the permeation rate parameters found varied (Table 5). In order to be able to quantify the skin permeation kinetics (by means of amounts collected at selected times in the receptor fluid), we used PG. This compound is an humectant and co-solvent, commonly used in dermal application, but also considered a permeation enhancer. For these reasons, we have selected this compound to be added to the gel formulations, in order to obtain detectable values in the receptor fluid, and hence, quantify the kinetic parameters.

When comparing the variable gelling excipients containing dispersed TH-NLCs, the highest penetration values were observed for GC-TH-NLCs and GH-TH-NLCs. However, HPMC increased the penetration kinetics (flux and K_p) compared to the carbomer, although, these values were not statistically significant between them. Comparing the total amount retained inside the skin, GC-TH-NLCs and GH-TH-NLCs obtained higher and similar values, which were statistically significant compared to those of GP-TH-NLCs ($p < 0.0001$) (Figure 6A). In the case of GP, this gel type exhibited a very slow penetration rate with statistically significant differences ($p < 0.01$). However, it provides a sticky gel film on the skin with lower spreading ability, resulting in very low amounts retained inside the skin. However, comparing

Table 4 Kinetics Release of TH Adjusted to Hyperbole Equation and Comparison of the Total Amount Released (Q_r) in 24 H. Data are Expressed as Mean \pm SD

$\frac{dQ}{dt} = \frac{V_m \cdot Q}{K_m + Q}$				
	TH	TH-NLC	GC-TH	GC-TH-NLC
V_m	517.6 \pm 14.16	1218.0 \pm 141.5 a c	399.7 \pm 8.09	1673.0 \pm 290.3 a c
K_m	4.543 \pm 0.46	80.39 \pm 17.13 a c	1.102 \pm 0.059	148.7 \pm 19.91 a c
r^2	0.9971	0.9948	0.9997	0.9992
$Q_{r_24h_}(\mu g)$	420.1 \pm 41.9	284.3 \pm 28.1 a c	382.5 \pm 38.2	225.0 \pm 22.4 a c
SSD ($p < 0.05$)	a	b	c	d

Notes: Q_r : amount of TH released; t: time; V_m : maximum process speed; K_m : amount of TH relative to half of the maximum speed; k_d : dissociation constant; SSD: statistically significant differences (One-way ANOVA, Tukey's multiple comparison test). GC-TH indicates thymol dispersed in a carbomer gel and GC-TH-NLC indicates thymol loaded nanostructured lipid carriers dispersed in a carbomer gel.

Table 5 Ex vivo Skin Penetration Parameters of TH-NLC in Gel Formulations (CG-TH-NLC, GH-TH-NLC and GP-TH-NLC)

Parameter	GC-TH-NLC	GH-TH-NLC	GP-TH-NLC
J ($\mu g/cm^2/h$)	2.79 \pm 0.66	3.47 \pm 0.14	1.25 \pm 0.21 a b
K_p (cm^2/h)	1.11E-03 \pm 2.66E-04	1.39E-03 \pm 5.50E-05	5.00E-04 \pm 8.25E-05 a b
Q_p ($\mu g/cm^2$)	85.50 \pm 3.91 b	109.45 \pm 9.21	48.70 \pm 3.54 a b
SSD ($p < 0.01$)	a	b	c

Notes: J : flux; K_p : permeability constant; Q_p : total amount penetrated; SSD: statistically significant differences (One-way ANOVA, Tukey's multiple comparison test). GC-TH-NLC indicates thymol loaded nanostructured lipid carriers dispersed in a carbomer gel, and GH-TH-NLC indicates thymol loaded nanostructured lipid carriers dispersed in a hydroxypropyl methylcellulose gel and GP-TH-NLC indicates thymol loaded nanostructured lipid carriers dispersed in a Pluronic gel.

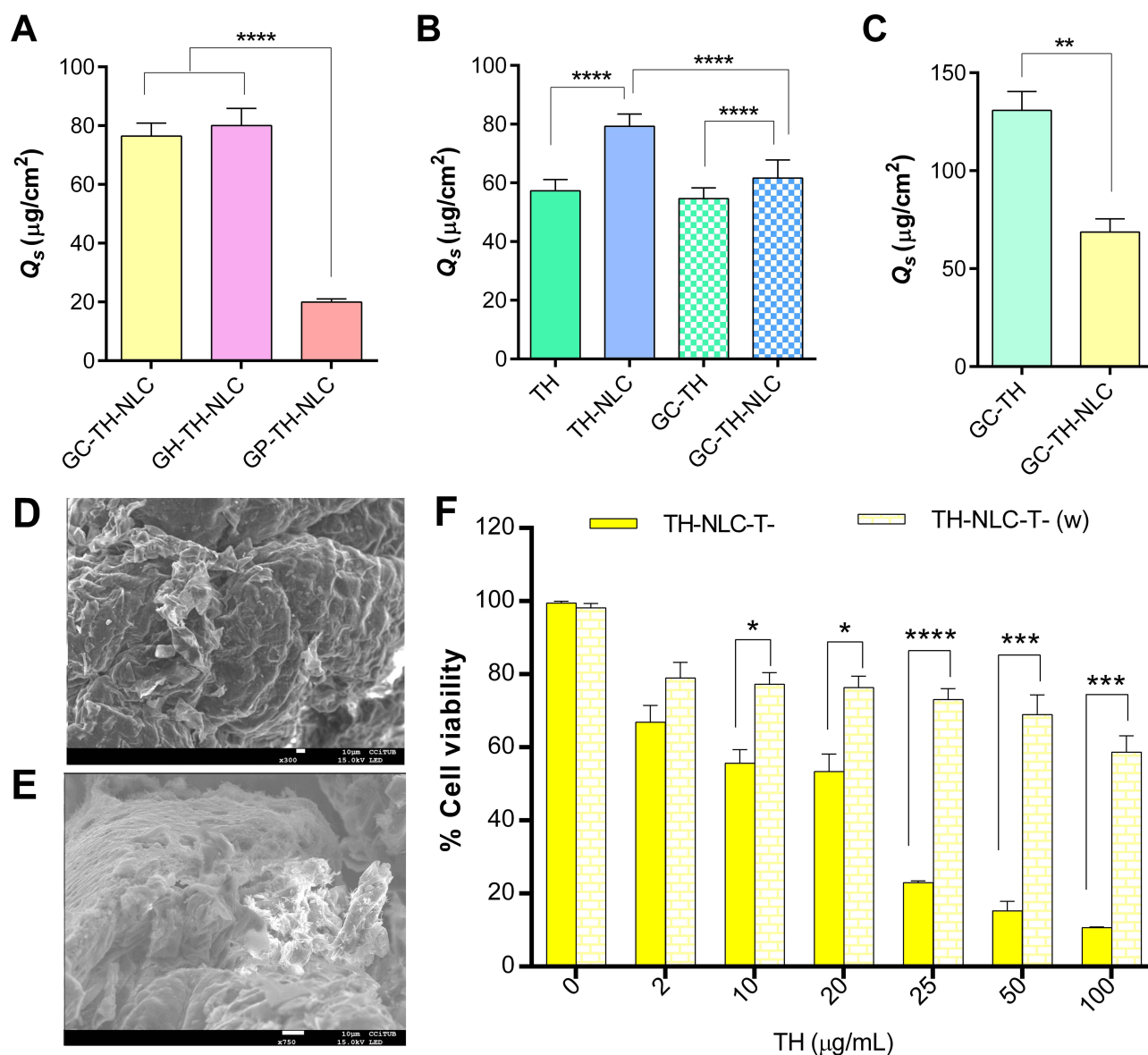


Figure 6 Ex vivo skin penetration for 24 h with quantification of the total amount retained inside the skin via extraction technique. (A) GC-TH-NLC, GH-TH-NLC and GP-TH-NLC (B), TH and TH-NLC aqueous and carbomer gels, (C) GC-TH and GC-TH-NLC (full-fat skin tissue). Data are expressed as mean \pm SD (n=3). SEM images of ex vivo human skin (D) untreated and (E) GC-TH-NLC permeation for 24 h. Scale bar: 10 μm (x300) and (x750), respectively. (F) Cell viability assay performed by MTT in HaCaT-cell lines treated with TH-NLC and washed particles (TH-NLC-w). Statistical analysis (t-test) analyzed for each concentration (* $p < 0.05$, ** $p < 0.01$, *** $p < 0.001$, **** $p < 0.0001$).

GC and GH, their performance on skin penetration of TH-NLC was similar, providing more suitable results. Due to the fact that carbomer gels (GC-TH-NLC) show to increased skin TH-NLC retention and have the advantages of ease of spreading, wide viscosity intervals, good organoleptic characteristics, and very low concentrations needed,^{58,59} this gel was chosen for further penetration studies. Therefore, carbomer gel was also used to incorporate TH in its free form, and this was compared to aqueous free TH and TH-NLC (Figure 6B).

As shown in Table 6, TH-NLC showed a more sustained penetration rate compared to that of TH in aqueous forms, in this case, absent of any additional enhancer. Statistically significant differences were observed in the flux (J), permeation constant (K_p), and total amount penetrated within 24 h (Q_p). In contrast, the permeation parameters obtained for the carbomer gels were similar for the GC-TH and GC-TH-NLCs, with no statistically significant differences between them. Moreover, the amount retained inside the skin was found to be higher for TH-NLC (aqueous and gel) than for TH, presenting statistically significant differences (Figure 6B).

Table 6 Ex vivo Skin Penetration Parameters of TH and TH-NLC Aqueous and Carbomer Gels

Parameter	TH	TH-NLC	GC-TH	GC-TH-NLC
J ($\mu\text{g}/\text{cm}^2/\text{h}$)	9.36 ± 0.31 b c d	1.66 ± 0.35 c d	2.53 ± 0.77	2.50 ± 0.06
K_p (cm^2/h)	$3.74\text{E-}03 \pm 1.240\text{E-}04$ b c d	$6.66\text{E-}04 \pm 1.39\text{E-}04$ c d	$1.01\text{E-}03 \pm 3.08\text{E-}04$	$9.9\text{E-}04 \pm 2.25\text{E-}05$
Q_p ($\mu\text{g}/\text{cm}^2$)	85.45 ± 9.63 b c d	42.34 ± 3.20 c d	38.79 ± 2.98	34.50 ± 4.53
SSD ($p < 0.01$)	a	b	c	d

Notes: J: flux; K_p : permeability constant; Q_p : total amount penetrated; SSD: statistically significant differences (One-way ANOVA, Tukey's multiple comparison test). GC-TH indicates thymol dispersed in a carbomer gel and GC-TH-NLC indicates thymol loaded nanostructured lipid carriers dispersed in a carbomer gel.

An additional study was developed using different skin donors than in the previous experiments, and the full skin layers, including the fat tissue, were used (1 mm thick) to access information on the penetration depth until the hypodermis. The TH and TH-NLC dispersed in carbomer gels were compared. The total amount of GC-TH found in the receptor fluid was significantly higher than that in the GC-TH-NLCs (Table 7). Moreover, the total amount retained inside the skin (Figure 6C) was significantly higher for GC-TH, which may indicate that free TH can be retained inside the fat tissue and attain blood circulation in a rapid manner, which is not convenient for this application. However, GC-TH-NLCs were retained only along the epidermis and dermis layers, resulting in a lower total amount found inside the total skin sample.

The skin penetration performed in fresh human explants by SEM is illustrated qualitatively in Figure 6D and 6E. A skin image (control) is shown in Figure 6D and the GC-TH-NLC matrix penetrating the skin tissue is shown in Figure 6E.

In vitro Cell Viability of TH-NLCs

The cell viability was assayed in HaCaT-cell line (human epidermal keratinocyte) using MTT for TH-NLC and also the same particles washed thrice to remove the excess of TW (TH-NLC-w). Figure 6F shows that the cytotoxicity of TH-NLC was dose dependent. However, after removing excess TW, cell viability was significantly increased ($p < 0.05$). Similar results were obtained for our previously developed thymol nanoparticles using TW.³¹ In fact, the occlusive properties of NLCs must be taken into account at the cellular level as well, since they are delivered directly onto the cell-culture monolayer along 24 h.

In vitro Antimicrobial Efficacy of TH-NLC

The antimicrobial activity was evaluated by calculating the MIC and D. MIC against *C. acnes* showed the same value for TH and TH-NLC at 250 $\mu\text{g}/\text{mL}$. This demonstrated that the TH-NLC were able to preserve TH activity by guaranteeing prolonged release. Moreover, the time to reduce 1/10 of the initial microbial concentration was evaluated at different dilutions. Therefore, the effect of the TH-NLC was slightly more sustained than that of TH (Figure 7A–7C).

Table 7 Ex vivo Skin Penetration Parameters of GC-TH versus GC-TH-NLC Using Full-Fat Skin Tissue

Parameter	GC-TH	GC-TH-NLC
J ($\mu\text{g}/\text{cm}^2/\text{h}$)	n.t	n.t
K_p (cm^2/h)	n.t	n.t
Q_p ($\mu\text{g}/\text{cm}^2$)	33.56 ± 3.67	$23.75 \pm 1.75^*$

Notes: J: flux; K_p : permeability constant; Q_p : total amount penetrated; n.t: not tested; $*p < 0.05$. GC-TH indicates thymol dispersed in a carbomer gel and GC-TH-NLC indicates thymol loaded nanostructured lipid carriers dispersed in a carbomer gel.

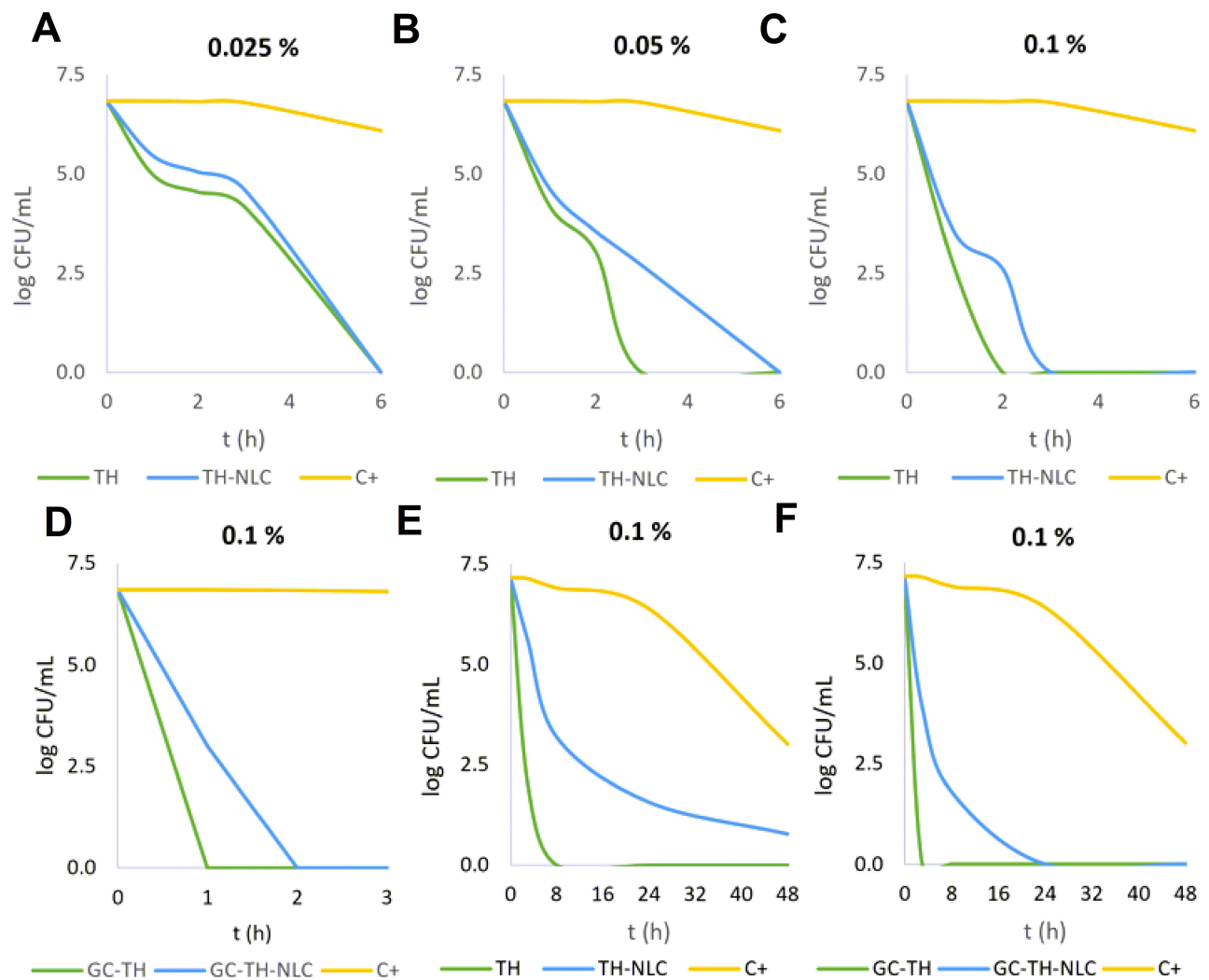


Figure 7 Bacterial viability assay with *C. acnes* inoculated with (A) TH and TH-NLC at 0.25 mg/mL up to 6 h, (B) TH and TH-NLC at 0.50 mg/mL up to 6 h, (C) (A) TH and TH-NLC at 1 mg/mL up to 6 h; (D) GC-TH and GC-TH-NLC for 3 h (at 1 mg/mL); and *S. epidermidis* inoculated for 48 h with 1 mg/mL of (E) TH and TH-NLC and (F) GC-TH and GC-TH-NLC.

However, when the formulations were incorporated into carbomer gels, slightly faster antimicrobial activity was observed (Figure 7D). In fact, when evaluating the release and permeation kinetics of the gels, comparing with their respective aqueous forms, it is clear that the activity in vivo will be more sustained, specifically for the encapsulated TH, being more favorable for the desired efficacy of the treatment, where the controlled release will aid to decrease dosage along time, not disturbing the entire skin microbiome.

For *S. epidermidis*, the activity of TH was rapid, whereas that of TH-NLC was highly sustained. TH achieved complete abolishment of the microorganism within 8 h, whereas TH-NLC still presented bacterial viability after 48 h (Figure 7E). Similar results were obtained for the carbomer gels, although the effect was slightly stronger in both cases, where bacterial viability was depleted within 3 h and 24 h for GC-TH and GC-TH-NLCs, respectively (Figure 7F).

The data for D are presented in Table 8. The kinetic data presented statistically significant differences for TH-NLC against TH for each evaluated dosage and microorganism ($p < 0.05$ and $p < 0.0001$) for *C. acnes* and *S. epidermidis*. The results showed that TH-NLC are more efficient in slowly reducing *C. acnes* viability, although they possess lower antimicrobial activity against *S. epidermidis*, compared to TH. These results are favorable for maintaining a healthy skin microbiota along with acne treatment.

Table 8 Decimal Reduction Time Data for *C. Acnes* and *S. Epidermidis* Treated with TH or TH-NLC

	mg/mL	r ²	Slope	D (Min)	SSD
C. acnes					
TH TH-NLC	0.25	0.9948 0.9763	-1.645 ± 0.1184 0.7629 ± 0.1188	36.47 ± 2.63 78.65 ± 12.25	**p < 0.01
TH TH-NLC	0.5	0.9960 0.9817	2.256 ± 0.1435 1.421 ± 0.1942	26.60 ± 1.69 42.22 ± 5.77	*p < 0.05
TH TH-NLC	1	0.9810 0.9973	3.425 ± 0.4763 2.261 ± 0.1175	17.52 ± 2.44 26.54 ± 1.38	**p < 0.01
S. epidermidis					
TH TH-NLC	1	0.9944 0.9913	1.744 ± 0.1311 0.5130 ± 0.03395	34.40 ± 2.59 116.96 ± 7.74	****p < 0.0001

Notes: *indicates $p < 0.05$, **indicates $p < 0.01$, ***indicates $p < 0.0001$.

Abbreviations: SSD, Statistically significant differences (one-way ANOVA, t-test).

Ex vivo Skin Antimicrobial Efficacy of TH-NLC

The antimicrobial activities of TH and TH-NLC were evaluated ex vivo using porcine skin. In every study performed, all formulations showed significant bacterial reduction compared to the control ($p < 0.0001$). The results of the prevention or treatment of antimicrobial effects are shown in Figure 8A. In both cases, better antimicrobial activity was obtained for prevention than treatment. In both protocols, the effect of TH-NLC was slightly higher than that of TH, and statistically significant differences were observed in the prevention study. On the other hand, when comparing the doses applied (Figure 8B), it can be observed that TH-NLC significantly increased the activity, with each additional dose applied, compared to a single dose. Meanwhile, TH was significant only after applying a 3-fold-dose increase. Comparing TH-NLC with TH at the same dose, a single administration did not show any differences between them. However, after multiple applications of each formulation, antimicrobial activity was statistically different. This can be explained by the rate of skin penetration, which agrees with the results of the present study. TH rapidly penetrated the skin layers, and TH-

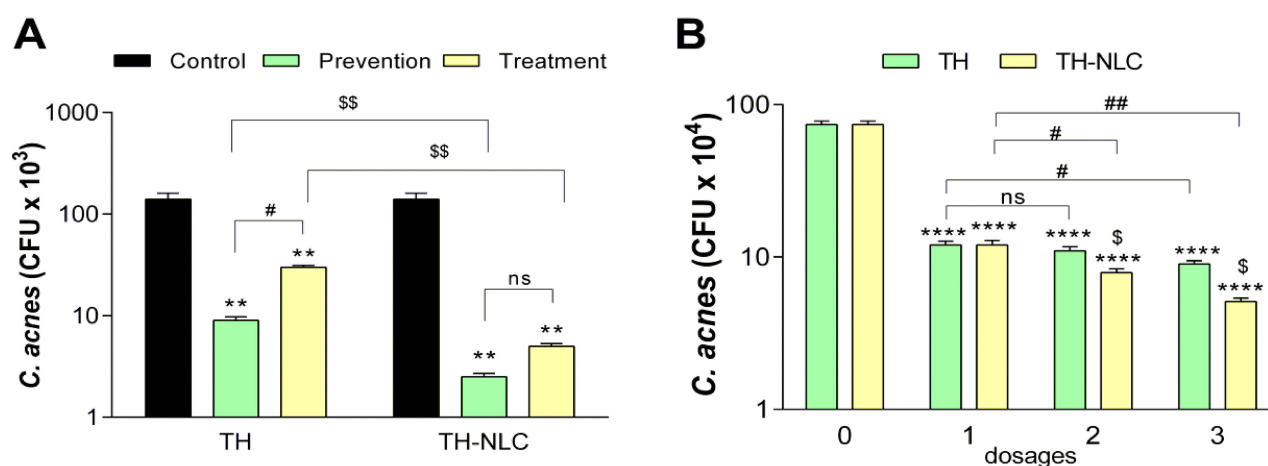


Figure 8 Bacteria viability on ex vivo treated skin with TH or TH-NLC for 24 h. Values represent viable count of *C. acnes* as the Mean \pm SD ($n=3$). **(A)** Prevention and treatment assessments. Statistical analysis was performed with one-way ANOVA Tukey's Multiple Comparison Test. **indicates $p < 0.01$ compared to control; \$ indicates $p < 0.01$ comparing TH and TH-NLC and # indicates $p < 0.05$ comparing prevention versus treatments. **(B)** Dose-dependent with 3 applied doses at times 0, 12 and 18 h of incubation. Statistical significance are represented as: *** $p < 0.0001$ treated groups compared to control; \$ $p < 0.05$ are comparing TH and TH-NLC (at the same dose); unpaired t-test carried out are represented as # indicates $p < 0.05$ and ## indicates $p < 0.01$ comparing multiple doses against single dose.

NLC permeability was sustained. Therefore, within 24 h of the total treatment period with multiple dosages, TH can be released from TH-NLC inside the skin, resulting in prolonged and higher activity compared to non-encapsulated TH.

Discussion

In this study, a formulation loaded with TH based on the last generation of lipid nanoparticles was developed, optimized, and dispersed in a gel matrix. Therefore, TH-loaded NLCs were successfully optimized. The solubility of TH in PCCG was higher than that in CCCG; therefore, PCCG was selected as the liquid lipid. Additionally, it presented less variability in the melting point, whereas the CCCG showed a higher temperature displacement. Moreover, two different preparation methods, HPH and US, had been used and compared. Observing the results obtained Z_{av} and PI were lower when HPH was used. However, there were no significant differences compared to the US method. The optimization of TH-NLC was based on the best solubility of TH in the liquid lipid, as well as the best values of Z_{av} and PI, by adjusting the correct concentration of TW. Moreover, TH-NLC optimized formulation presented minimal variations among the preparation methods. Observing the DoE, Z_{av} was smaller for 80:20 and 70:30, than for 60:40 GBH:PCCG proportions. This could be attributed to their medium-soft structures compared with their soft structures. The best values were found at 70:30 at TW levels 0 and +1, and the PI increased at levels -1 and +1 compared to 0, which must be due to the correct proportion of lipids and surfactant. The EE values were found in the range of 75–82%, and the highest was found for the central point. This is because of the correct proportion of lipids and surfactants that stabilize the system and encapsulate the active substance. The analysis of the results obtained led to an optimized formulation with an average size around 260 nm and a PI below 0.2, with more than 80% of TH encapsulated. Previous authors have also found that NLCs produced with HPH presented smaller Z_{av} and PI, than those produced with US, presented in two different articles.^{37,60} Moreover, a similar finding with their work was that the proportion of 70:30 (SL:LL) with the highest amount of TW presented the lower PI using US.⁶⁰

Gel formulations of TH-NLC have been developed using different gelling agents and viscosities. Carbomer and HPMC gels exhibit pseudoplastic flow behaviour, which is suitable for cosmetic formulations to achieve good spreading ability on the skin (Lee et al, 2009). On the other hand, Pluronic gels exhibit plastic flow behaviours, which can also explain the sensorial plastic film, presenting a dry opaque and rough appearance, formed on the skin surface when applied.⁴⁵ The sensorial properties of skin products are highly relevant for their applications, depending on the strategy developed. Therefore, it is important to test different vehicles and study their rheological behaviour, in order to provide the most suitable characteristics for the treatment and application.

The short-term stability of the developed TH-NLC, showed broad variability in the backscattering signals measured for the TH-NLC. However, when incorporated into gel formulations (GC-TH-NLCs), this phenomenon was stabilized. The sterility of the GC-TH-NLCs was confirmed by testing the microbial growth of bacteria, fungi, and yeast, which were absent after 12 months of storage at RT. For this reason, TH has provided microbial preservative activity for gel formulations, which is in agreement with other authors.⁶¹ In addition, the morphology of TH-NLC was analyzed by TEM, which showed a semi-spherical soft shape, characteristic of this type of nanocarrier.³⁶

The *in vitro* release of TH-NLC was sustained being similar for its aqueous and gel formulations, whereas TH presented a fast release, also similar for its both formulation types. In fact, there were statistically significant differences found for TH compared to TH-NLC ($p < 0.01$) and GC-TH-NLC ($p < 0.001$), as well as for GC-TH compared to TH-NLC ($P < 0.05$) and GC-TH-NLC ($p < 0.01$), data analysed at 24 h. In the other hand, TH vs GC-TH or TH-NLC vs GC-TH-NLC comparison were not significant, meaning that both products (free or encapsulated) present similar release kinetics as both formulation types (aqueous and gel). Therefore, the fast release of TH can be observed independent of the vehicle, meanwhile, the sustained release of TH-NLC is also maintained when found as gel formulation. This means that our developed carbomer gel excipients do not alter the release nature of the products.

Skin permeation kinetics (flux and permeation constant) of TH-NLC were slower than that of free TH, which agrees with the prolonged release of TH-NLCs. In the case of the carbomer gel formulations, data were similar for both (GC-TH and GC-TH-NLC), presenting significant differences compared to their aqueous forms. The highest amount found in the receptor fluid was for TH, presenting significant differences ($p < 0.0001$) compared with all other formulations. TH is also considered a penetration enhancer compound, and under *ex vivo* evaluation, differences in penetration parameters can be observed.⁶² Moreover, the total amount found inside the skin was significantly higher for the TH-NLC than for the TH. Also, the amount of

GC-TH-NLC was slightly higher than that of GC-TH, although the difference was not statistically significant. When comparing the permeation of TH-NLC in several gel formulations, carbomer vehicles presented slower skin permeation rates than HPMC but faster than Pluronic. In fact, GC-TH-NLCs and GH-TH-NLCs retained similar amounts inside the skin, which was statistically significant compared to GP-TH-NLCs. Since lipid nanoparticles are known to perform fill-forming on the skin surface, they can also delay entry across the entire skin depth. Other authors have also confirmed that carbomers and HPMC are suitable vehicles for NLC gel formulations.⁵⁸ On the other hand, Pluronic presents thermo-reversible gelling properties between room temperature and body temperature, which may benefit dermal applications. For this reason, the gel became thicker in contact with the skin, presenting increased bioadhesive properties and providing an even more sustained permeation of TH-NLC, which was statistically significant compared to the other gels ($p < 0.001$ and $p < 0.0001$, for GC-TH-NLC and GH-TH-NLC, respectively). In a study performed with full skin thickness, including the fat tissue, the total amount of TH found in the receptor fluid for GC-TH and GC-TH was similar, whereas the total amount retained inside the skin was higher for GC-TH than for GC-TH-NP. This may be attributed to the fact that the TH-NLC dispersed in the gel were retained along the epidermis and dermis layers, resulting in a lower total amount found inside the total skin sample. Previous authors have stated that fat tissue may serve as a deep compartment for the drug, delaying its entry into the blood.⁶³ Therefore, this increases the time retained inside the target skin layer. Additionally, considering that glycerin and propylene glycol are used in cosmetics formulations at 0–50% as solubilizer or viscosity decreasing agent, but most commonly found at 1–5% as humectant, conditioning agent, among other properties,^{64,65} there have been several studies reporting the use of PG as skin penetration enhancers.^{66–69} In this work, we have selected this type of compounds to evaluate the penetration capacity of gels containing TH or TH-NLC, considering that TH is also a skin penetration enhancer, to compare both dermal excipients. When evaluating their aqueous form, absent of additional ingredients, the skin penetration rate of TH was extremely faster (5.6X). When we tested the gel formulations containing TH-NLCs, we could obtain high amounts retained inside the skin, but not enough amounts in the receptor fluid, which is a positive effect, since they remain inside the skin, not reaching the systemic circulation. For this reason, we formulated all the gel dosage forms with PG, to be able to collect data from the receptor fluid and calculate the skin permeation kinetics, to compare the variable behavior among the excipients tested. Thus, comparing GC-TH vs GC-TH-NLC under these conditions, we have found that the permeation rate was similar for both formulations, however, still presenting higher amounts of retained inside the skin for GC-TH-NLC. Nevertheless, we have studied the permeation of the gels using full-skin sample containing the fat layer and we found that, in this case, the amount inside the skin was higher for GC-TH, considering that the fat tissue acts as a deep compartment for the nanoparticles, while TH rapidly reaches the underlying tissues, as well as reaching the blood circulation.⁶³ Based on these findings, we have encapsulated TH into NLC to successfully maintain TH release inside the skin, slowly and prolonged and with the aim to be retained near the hair follicle, and therefore, lower dosages can be applied, resulting in higher activity designed for acne treatment.

The cell viability assay performed on HaCaT cells showed that the developed TH-NLC were cytotoxic at high doses. However, at lower doses and removal of excess free TW from the formulation, cell viability increased significantly. Previous studies have reported that the cytotoxicity of lipid NPs in HaCaT cells is dependent on surfactant type and concentration.⁷⁰ Additionally, other authors have stated that lipid NPs cytotoxicity may be attributed to lipid peroxidation and ROS generation, depending on the cell type and concentration used.⁷¹ In addition, previously developed polymeric nanoparticles of thymol using Tween 20 as stabilizer at 0.4% (four times lower than of the present TH-NLC) showed no cytotoxicity in HaCaT cells at the same concentrations studied (2–100 $\mu\text{g/mL}$), presenting only significant differences between washed and non-washed particles at 100 $\mu\text{g/mL}$.³¹ Therefore, the lipidic structure and a higher amount of TW required slightly lower doses to obtain higher cell viability. Nevertheless, the most important is that TH-NLCs formulations were not cytotoxic, and additionally, their slow-rate penetration inside the skin would also provide lower concentrations without reaching systemic circulation, being considered as safe.

The antimicrobial activity of TH-NLCs against *C. acnes* was slightly higher than that of TH. There were statistically significant differences ($p < 0.01$, $p < 0.05$ and $p < 0.01$) for the decimal reduction times for each dosage (0.25, 0.5 and 1 mg/mL), being 2X, 1.6X and 1.5X times slower, respectively. When the gel formulations were applied at 1 mg/mL , the activity was similar to that of the aqueous forms, but slightly faster effects were observed for their gels (GC-TH and GC-TH-NLC). When comparing the formulations, aqueous and carbomer gels, against *S. epidermidis* (at 2X MIC), both formulations presented a prolonged time to detain microorganism viability compared to *C. acnes* (at 4X MIC). Moreover,

the time taken to reduce bacterial viability was found to be 3.4 times slower for the TH-NLC than for the TH. Therefore, the results obtained demonstrated the efficacy of TH-NLC in efficiently decreasing *C. acnes* proliferation without affecting the aggressiveness of the skin microbiota. Moreover, these findings can also be associated with the slow-rate release of TH-NLCs, and additionally, by counting with a slow-rate skin penetration, the mild anti-microbial activity would be prolonged as more efficient.

Ex vivo antimicrobial activity has been successfully investigated in human skin explants for prevention and treatment. The antimicrobial activity of the TH-NLCs was found higher than that of TH. In the study of multiple doses applied, there were only significant differences for TH when comparing the three doses with a single dose ($p < 0.05$). However, for TH-NLC, there were statistically significant differences at each multiple doses applied compared with a single dose ($p < 0.05$ and $p < 0.01$ for the second and third dosage, respectively). These results agree with the skin permeation parameters, where the TH-NLC can be maintained for a longer time inside the skin, whereas TH penetrates across all layers in a fast manner. Therefore, long-term treatment is expected to provide more efficient results with TH-NLC than with TH alone. Therefore, the development TH-NLCs can be considered a great approach for a natural skin treatment, avoiding the use of antibiotics as active ingredients, as well as the need of strong chemical molecules as cosmetic preservative.

Nevertheless, TH is also an antioxidant molecule, therefore, when used in cosmetic formulations, along time it may oxidize to preserve other compounds. It has also been also used as cosmetic preservative due to its antimicrobial properties.^{61,72} Moreover, due to TH antioxidant properties, its encapsulation is highly recommended to extend their shelf-life. For these reasons, there has also been a variety of recent research developing TH-loaded NLC structures providing antimicrobial and antioxidant activity.^{73–75} In fact, those are all mainly applied to the food industry as antioxidants and preservatives. Although, these were all made of lipid mixtures of non-pure nature, where they also contained a variety of others nutritional ingredients inside its composition, such as proteins and sugars, among others, proving completely different characteristics than those for cosmetics applications. Additionally, in food science, the antimicrobial activity for food additive must abolish the micro-organism, in order to act as a food preservative, since nutritional components must not present living pathogens, to avoid food poisoning. In contrast, when dealing with an antimicrobial for skin treatment, the activity must not be so aggressive eradicating all living organisms, since there is a microbiome system which maintains the skin optimal functions. Meanwhile, our work is based on natural products, all based on plant origin or synthetic origin (non-animal) and the ingredients used are pure grade, making our product a simple and efficient formulation, suitable for topical acne treatment. Moreover, our production method only used water as solvent, without organic solvents, being a natural and sustainable fabrication. Furthermore, all the ingredients were sustainable and from non-animal sources.

Conclusions

In this study, a nanostructured carrier capable of encapsulating thymol, a natural compound, for the treatment of *Acne vulgaris* was developed and optimized. Therefore, thymol was loaded into nanostructured lipid carriers possessing emollient and moisturizing properties, and the formulation was optimized using a design of experiments approach. TH-NLC have been shown to provide a prolonged TH release. In addition, the TH-NLC and free TH were dispersed into several gelling formulations increasing NLC stability and showing to form gel threads with NLC embedded within them. Between all tested gels, carbomers were highly retained in skin tissues and provided a low permeation rate. In addition, carbomer gels provided a prolonged release up to 72 h and penetration parameters and therapeutic efficacy demonstrated their suitability for application in the skin against *Acne vulgaris* preserving the healthy skin microbiota, and being suitable for replacing antibiotic treatments.

Acknowledgments

The authors wish to acknowledge the support of the Spanish Ministry under project PID2021-122187NB-C32 and the support of the Generalitat of Catalonia (2017SGR1447). ESL wants to acknowledge the requalification system grants.

Disclosure

The authors report no conflicts of interest in this work.

References

- Williams HC, Dellavalle RP, Garner S. Acne vulgaris. *Lancet*. 2012;379(9813):361–372. doi:10.1016/S0140-6736(11)60321-8
- Sachdeva M, Tan J, Lim J, Kim M, Nadeem I, Bismil R. The prevalence, risk factors, and psychosocial impacts of acne vulgaris in medical students: a literature review. *Int J Dermatol*. 2021;60(7):792–798. doi:10.1111/ijd.15280
- Tayel K, Attia M, Agamia N, Fadl N. Acne vulgaris: prevalence, severity, and impact on quality of life and self-esteem among Egyptian adolescents. *J Egypt Public Health Assoc*. 2020;95(1). doi:10.1186/s42506-020-00056-9
- Thiboutot D, Del Rosso JQ. Acne vulgaris and the epidermal barrier: is acne vulgaris associated with inherent epidermal abnormalities that cause impairment of barrier functions? Do any topical acne therapies alter the structural and/or functional integrity of the epidermal barrier? *J Clin Aesthet Dermatol*. 2013;6(2):18–24.
- Bhatia A, Maisonneuve JF, Persing DH. Propionibacterium Acnes and chronic diseases. In: *The Infectious Etiology of Chronic Diseases: Defining the Relationship, Enhancing the Research, and Mitigating the Effects: Workshop Summary*. The National Academies Press; 2004.
- Claudel JP, Auffret N, Leccia MT, Poli F, Corvec S, Dréno B. Staphylococcus epidermidis: a potential new player in the physiopathology of acne? *Dermatology*. 2019;235(4):287–294. doi:10.1159/000499858
- Boukraâ L, Abdellah F, Ait-Abderrahim L. Antimicrobial properties of bee products and medicinal plants microbial pathogens and strategies for combating them: science, technology and education. *Formatex*. 2013;2013:960–970.
- Grice EA, Segre JA. The skin microbiome. *Nat Rev Microbiol*. 2011;9(4):244–253. doi:10.1038/nrmicro2537
- Otto M. Staphylococcus epidermidis – the “accidental” pathogen. *Nat Rev Microbiol*. 2009;7(8):557–567. doi:10.1038/nrmicro2182
- Briganti S, Picardo M. Antioxidant activity, lipid peroxidation and skin diseases. What’s new. *J Eur Acad Dermatol Venereol*. 2003;17(6):663–669. doi:10.1046/j.1468-3083.2003.00751.x
- Escobar A, Pérez M, Romanelli G, Blustein G. Thymol bioactivity: a review focusing on practical applications. *Arab J Chem*. 2020;13(12):9243–9269. doi:10.1016/j.arabjc.2020.11.009
- Sahoo CR, Paidesetty SK, Padhy RN. The recent development of thymol derivative as a promising pharmacological scaffold. *Drug Dev Res*. 2021;82(8):1079–1095. doi:10.1002/ddr.21848
- Mozafari MR, Alavi M Micro Nano Bio Aspects. 2023;10–13.
- Liu Y, Yan H, Yu B, et al. Protective effects of natural antioxidants on inflammatory bowel disease: thymol and its pharmacological properties. *Antioxidants*. 2022;11(10):1947. doi:10.3390/antiox11101947
- Nagoor Meeran MF, Jagadeesh GS, Selvaraj P. Thymol, a dietary monoterpene phenol abrogates mitochondrial dysfunction in β -adrenergic agonist induced myocardial infarcted rats by inhibiting oxidative stress. *Chem Biol Interact*. 2016;244:159–168. doi:10.1016/j.cbi.2015.12.006
- Najafloo R, Behyari M, Imani R, Nour S. A mini-review of Thymol incorporated materials: applications in antibacterial wound dressing. *J Drug Deliv Sci Technol*. 2020;60(March). doi:10.1016/j.jddst.2020.101904
- Pivetta TP, Simões S, Araújo MM, Carvalho T, Arruda C, Marcato PD. Development of nanoparticles from natural lipids for topical delivery of thymol: investigation of its anti-inflammatory properties. *Colloids Surf B Biointerfaces*. 2018;164:281–290. doi:10.1016/j.colsurfb.2018.01.053
- Alvarez-Román R, Naik A, Kalia YN, Guy RH, Fessi H. Skin penetration and distribution of polymeric nanoparticles. *J Control Release*. 2004;99(1):53–62. doi:10.1016/j.jconrel.2004.06.015
- Mahmoud K, Swidan S, El-Nabarawi M, Teaima M. Lipid based nanoparticles as a novel treatment modality for hepatocellular carcinoma: a comprehensive review on targeting and recent advances. *J Nanobiotechnology*. 2022;20(1):1–42. doi:10.1186/s12951-022-01309-9
- Rincón M, Espinoza LC, Silva-Abreu M, et al. Quality by design of pranoprofen loaded nanostructured lipid carriers and their ex vivo evaluation in different mucosae and ocular tissues. *Pharmaceuticals*. 2022;15(10). doi:10.3390/ph15101185
- Wang L, Zhao X, Zhu C, et al. Thymol kills bacteria, reduces biofilm formation, and protects mice against a fatal infection of Actinobacillus pleuropneumoniae strain L20. *Vet Microbiol*. 2017;203:202–210. doi:10.1016/j.vetmic.2017.02.021
- Gu Y, Yang M, Tang X, et al. Lipid nanoparticles loading triptolide for transdermal delivery: mechanisms of penetration enhancement and transport properties. *J Nanobiotechnology*. 2018;16(1):1–14. doi:10.1186/s12951-018-0389-3
- Khater D, Nsairat H, Odeh F, et al. Transdermal Lipid Nanoparticles: a Review; 2021:1–43.
- Slavkova M, Tzankov B, Popova T, Voycheva C. Gel formulations for topical treatment of skin cancer: a review. *Gels*. 2023;9(5). doi:10.3390/gels9050352
- Mohd Ariffin NH, Hasham R. Assessment of non-invasive techniques and herbal-based products on dermatological physiology and intercellular lipid properties. *Heliyon*. 2020;6(5). doi:10.1016/j.heliyon.2020.e03955
- Yamamoto A, Takenouchi K, Ito M. Impaired water barrier function in acne vulgaris. *Arch Dermatol Res*. 1995;287(2):214–218. doi:10.1007/BF01262335
- Yolanda MO, Jusuf NK, Putra IB. Lower facial skin hydration level increases acne vulgaris severity level. *Bali Med J*. 2021;10(3):1081–1084. doi:10.15562/bmj.v10i3.2195
- Souto EB, Baldim I, Oliveira WP, et al. SLN and NLC for topical, dermal, and transdermal drug delivery. *Expert Opin Drug Deliv*. 2020;17(3):357–377. doi:10.1080/17425247.2020.1727883
- Mishra S, Kesharwani R, Tiwari AK, Patel DK. Improvement of drug penetration through the skin by using Nanostructured Lipid Carriers (NLC). *Int J Pharm Pharm Res*. 2016;6(3):481–496.
- Lauterbach A, Müller-Goymann CC. Applications and limitations of lipid nanoparticles in dermal and transdermal drug delivery via the follicular route. *Eur J Pharm Biopharm*. 2015;97:152–163. doi:10.1016/j.ejpb.2015.06.020
- Folle C, Marqués AM, Diaz-Garrido N, et al. Thymol-loaded PLGA nanoparticles: an efficient approach for acne treatment. *J Nanobiotechnology*. 2021;19(1):359. doi:10.1186/s12951-021-01092-z
- Farsani PA, Mahjub R, Mohammadi M, Oliaei SS, Mahboobian MM. Development of perphenazine-loaded solid lipid nanoparticles: statistical optimization and cytotoxicity studies. *Biomed Res Int*. 2021;2021. doi:10.1155/2021/6619195
- Cavendish M, Nalane L, Barbosa T, et al. Study of pre-formulation and development of solid lipid nanoparticles containing perillyl alcohol. *J Therm Anal Calorim*. 2020;141(2):767–774. doi:10.1007/s10973-019-09080-0
- Gill P, Moghadam TT, Ranjbar B. Differential scanning calorimetry techniques: applications in biology and nanoscience. *J Biomol Tech*. 2010;21(4):167–193.

35. Gonzalez-Pizarro R, Silva-Abreu M, Calpena AC, Egea MA, Espina M, García ML. Development of fluorometholone-loaded PLGA nanoparticles for treatment of inflammatory disorders of anterior and posterior segments of the eye. *Int J Pharm.* **2018**;547:1–2.
36. Carvajal-Vidal P, Fábrega MJ, Espina M, Calpena AC, García ML. Development of Halobetasol-loaded nanostructured lipid carrier for dermal administration: optimization, physicochemical and biopharmaceutical behavior, and therapeutic efficacy. *Nanomed Nanotechnol Biol Med.* **2019**;20:102026. doi:10.1016/j.nano.2019.102026
37. Rincón M, Calpena AC, Clares B, et al. Skin-controlled release lipid nanosystems of pranoprofen for the treatment of local inflammation and pain. *Nanomedicine.* **2018**;13(19):2397–2413. doi:10.2217/nmm-2018-0195
38. Andersen A. Final report on the safety assessment of sodium p-Chloro-m-Cresol, p-Chloro-m-Cresol, Chlorothymol, Mixed Cresols, m-Cresol, o-Cresol, p-Cresol, Isopropyl Cresols, Thymol, o-Cymen-5-ol, and Carvacrol. *Int J Toxicol.* **2006**;25(Suppl 1):29–127. doi:10.1080/10915810600716653
39. McConnell ML. Particle size determination by quasielastic light scattering. *Anal Chem.* **1981**;53(8):1–5. doi:10.1021/ac00231a799
40. López-Machado A, Díaz N, Cano A, et al. Development of topical eye-drops of lactoferrin-loaded biodegradable nanoparticles for the treatment of anterior segment inflammatory processes. *Int J Pharm.* **2021**;609:121188. doi:10.1016/j.ijpharm.2021.121188
41. Sosa L, Calpena AC, Silva-Abreu M, et al. Thermoreversible gel-loaded amphotericin B for the treatment of dermal and vaginal candidiasis. *Pharmaceutics.* **2019**;11(7):1–18. doi:10.3390/pharmaceutics11070312
42. Lemarchand C, Couvreur P, Vauthier C, Costantini D, Gref R. Study of emulsion stabilization by graft copolymers using the optical analyzer Turbiscan. *Int J Pharm.* **2003**;254:77–82. doi:10.1016/S0378-5173(02)00687-7
43. Suñer-Carbó J, Boix-Montañés A, Halbaut-Bellowa L, et al. Skin permeation of econazole nitrate formulated in an enhanced hydrophilic multiple emulsion. *Mycoses.* **2017**;60(3):166–177. doi:10.1111/myc.12575
44. Abrego G, Alvarado H, Souto EB, et al. Biopharmaceutical profile of pranoprofen-loaded PLGA nanoparticles containing hydrogels for ocular administration. *Eur J Pharm Biopharm.* **2015**;95:261–270. doi:10.1016/j.ejpb.2015.01.026
45. Carvajal-Vidal P, González-Pizarro R, Araya C, et al. Nanostructured lipid carriers loaded with Halobetasol propionate for topical treatment of inflammation: development, characterization, biopharmaceutical behavior and therapeutic efficacy of gel dosage forms. *Int J Pharm.* **2020**;585:119480. doi:10.1016/j.ijpharm.2020.119480
46. Sarango-Granda P, Espinoza LC, Díaz-Garrido N, et al. Effect of penetration enhancers and safety on the transdermal delivery of apremilast in skin. *Pharmaceutics.* **2022**;14(5). doi:10.3390/pharmaceutics14051011
47. Limón D, Gil-Lianes P, Rodríguez-Cid L, et al. Supramolecular hydrogels consisting of nanofibers increase the bioavailability of curcuminoids in inflammatory skin diseases. *ACS Appl Nano Mater.* **2022**;5(10):13829–13839. doi:10.1021/acsanm.2c01482
48. Folle C, Díaz-Garrido N, Sánchez-López E, et al. Surface-modified multifunctional thymol-loaded biodegradable nanoparticles for topical acne treatment. *Pharmaceutics.* **2021**;13(9). doi:10.3390/pharmaceutics13091501
49. Alvarado HL, Abrego G, Souto EB, et al. Nanoemulsions for dermal controlled release of oleanolic and ursolic acids: in vitro, ex vivo and in vivo characterization. *Colloids Surf B Biointerfaces.* **2015**;130:40–47. doi:10.1016/j.colsurfb.2015.03.062
50. Messenger S, Hann AC, Goddard PA, Dettmar PW, Maillard JY. Use of the “ex vivo” test to study long-term bacterial survival on human skin and their sensitivity to antiseptics. *J Appl Microbiol.* **2004**;97(6):1149–1160. doi:10.1111/j.1365-2672.2004.02403.x
51. Díaz-Garrido N, Fábrega MJ, Vera R, Giménez R, Badia J, Baldomà L. Membrane vesicles from the probiotic Nissle 1917 and gut resident *Escherichia coli* strains distinctly modulate human dendritic cells and subsequent T cell responses. *J Funct Foods.* **2019**;61(May). doi:10.1016/j.jff.2019.103495
52. Koeth LM, Miller LA. Antimicrobial susceptibility test methods: dilution and disk diffusion methods. In: Carroll KC, Pfaller MA, Landy ML, Patel R, McAdam AJ, Richter S, editors. *Manu Clin Microbiol.* 12th ed. Washington D: ASM Press; **2019**: 1284–1299. doi:10.1128/9781683670438.MCM.ch73
53. MacGowan AP, Wootton M, Hedges AJ, Bowker KE, Holt HA, Reeves DS. A new time-kill method of assessing the relative efficacy of antimicrobial agents alone and in combination developed using a representative β -lactam, aminoglycoside and fluoroquinolone. *J Antimicrob Chemother.* **1996**;38(2):193–203. doi:10.1093/jac/38.2.193
54. Messenger S, Goddard PA, Dettmar PW, Maillard JY. Determination of the antibacterial efficacy of several antiseptics tested on skin by an “ex-vivo” test. *J Med Microbiol.* **2001**;50(3):284–292. doi:10.1099/0022-1317-50-3-284
55. Amasya G, Ozturk C, Aksu B, Tarimci N. QbD based formulation optimization of semi-solid lipid nanoparticles as nano-cosmeceuticals. *J Drug Deliv Sci Technol.* **2021**;66:102737. doi:10.1016/j.jddst.2021.102737
56. Souto EB, Almeida AJ, Müller RH. Lipid nanoparticles (SLN[®], NLC[®]) for cutaneous drug delivery: structure, protection and skin effects. *J Biomed Nanotechnol.* **2007**;3(4):317–331. doi:10.1166/jbn.2007.049
57. Sreevidya VS. An Overview on Emulgel. *Int J Pharm Phytopharm Res.* **2019**;9(1):92–97. doi:10.52711/2231-5691.2023.00037
58. Amasya G, Inal O, Sengel-Turk CT. SLN enriched hydrogels for dermal application: full factorial design study to estimate the relationship between composition and mechanical properties. *Chem Phys Lipids.* **2020**;228:3. doi:10.1016/j.chemphyslip.2020.104889
59. Gonzalez-Mira E, Nikolić S, Calpena AC, Egea MA, Souto EB, García ML. Improved and safe transcorneal delivery of flurbiprofen by NLC and NLC-based hydrogels. *J Pharm Sci.* **2012**;101(2):707–725. doi:10.1002/jps.22784
60. Rincón M, Calpena AC, Fabrega MJ, et al. Development of pranoprofen loaded nanostructured lipid carriers to improve its release and therapeutic efficacy in skin inflammatory disorders. *Nanomaterials.* **2018**;8(12). doi:10.3390/nano8121022
61. Manou I, Bouillard L, Devleeschouwer MJ, Barel AO. Evaluation of the preservative properties of Thymus vulgaris essential oil in topically applied formulations under a challenge test. *J Appl Microbiol.* **1998**;84(3):368–376. doi:10.1046/j.1365-2672.1998.00353.x
62. Pham QD, Björklund S, Engblom J, Topgaard D, Sparr E. Chemical penetration enhancers in stratum corneum - Relation between molecular effects and barrier function. *J Control Release.* **2016**;232:175–187. doi:10.1016/j.jconrel.2016.04.030
63. Calpena AC, Clares B, Fernández F. Technological, biopharmaceutical and pharmacokinetic advances: new formulations of application on the skin and oral mucosa. In: Muñoz-Torrero D, editor. *Recent Adv Pharmal Sci.* Vol. 661. Transworld Research Network; **2011**:175–198.
64. Becker LC, Bergfeld WF, V. BD, et al. Safety Assessment of Glycerin as Used in Cosmetics. *Int J Toxicol.* **2019**;38(3_suppl):6S–22S. doi:10.1177/1091581819883820
65. Fiume MM, Bergfeld WF. Safety assessment of propylene glycol, tripropylene glycol, and PPGs as used in cosmetics. *Int J Toxicol.* **2012**;31:245S–260S. doi:10.1177/1091581812461381

66. Russo J, Fiegel J, Brogden NK. Rheological and drug delivery characteristics of poloxamer-based diclofenac sodium formulations for chronic wound site analgesia. *Pharmaceutics*. **2020**;12(12):1–18. doi:10.3390/pharmaceutics12121214
67. Carrer V, Alonso C, Pont M, et al. Effect of propylene glycol on the skin penetration of drugs. *Arch Dermatol Res*. **2020**;312(5):337–352. doi:10.1007/s00403-019-02017-5
68. Giuliano E, Paolino D, Fresta M, Cosco D. Mucosal applications of poloxamer 407-based hydrogels: an overview. *Pharmaceutics*. **2018**;10(3):1–26. doi:10.3390/pharmaceutics10030159
69. Díez-Sales O, Garrigues TM, Herráez JV, Belda R, Martín-Villodre A, Herráez M. In vitro percutaneous penetration of acyclovir from solvent systems and carbopol 971-P hydrogels: influence of propylene glycol. *J Pharm Sci*. **2005**;94(5):1039–1047. doi:10.1002/jps.20317
70. Maupas C, Moulari B, Béduneau A, Lamprecht A, Pellequer Y. Surfactant dependent toxicity of lipid nanocapsules in HaCaT cells. *Int J Pharm*. **2011**;411(1–2):136–141. doi:10.1016/j.ijpharm.2011.03.056
71. Szwed M, Torgersen ML, Kumari RV, et al. Biological response and cytotoxicity induced by lipid nanocapsules. *J Nanobiotechnol*. **2020**;18(1):1–19. doi:10.1186/s12951-019-0567-y
72. Amiri H. Essential oils composition and antioxidant properties of three thymus species. *Evid Based Complement Altern Med*. **2012**;2012. doi:10.1155/2012/728065
73. Karimi-Khorrami N, Radi M, Amiri S, Abedi E, McClements DJ. Fabrication, characterization, and performance of antimicrobial alginate-based films containing thymol-loaded lipid nanoparticles: comparison of nanoemulsions and nanostructured lipid carriers. *Int J Biol Macromol*. **2022**;207:801–812. doi:10.1016/j.ijbiomac.2022.03.149
74. Baqeri F, Nejatian M, Abbaszadeh STM. The effect of gelatin and thymol-loaded nanostructured lipid carrier on physicochemical, rheological, and sensory properties of sesame paste/date syrup blends as a snack bar. *J Texture Stud*. **2020**;51(3):501–510.
75. Sepahvand S, Amiri S, Radi M, Amiri MJ. Effect of Thymol and Nanostructured Lipid Carriers (NLCs) Incorporated with Thymol as Antimicrobial Agents in Sausage. *Sustain*. **2022**;14(4). doi:10.3390/su14041973

International Journal of Nanomedicine

Dovepress

Publish your work in this journal

The International Journal of Nanomedicine is an international, peer-reviewed journal focusing on the application of nanotechnology in diagnostics, therapeutics, and drug delivery systems throughout the biomedical field. This journal is indexed on PubMed Central, MedLine, CAS, SciSearch®, Current Contents®/Clinical Medicine, Journal Citation Reports/Science Edition, EMBase, Scopus and the Elsevier Bibliographic databases. The manuscript management system is completely online and includes a very quick and fair peer-review system, which is all easy to use. Visit <http://www.dovepress.com/testimonials.php> to read real quotes from published authors.

Submit your manuscript here: <https://www.dovepress.com/international-journal-of-nanomedicine-journal>